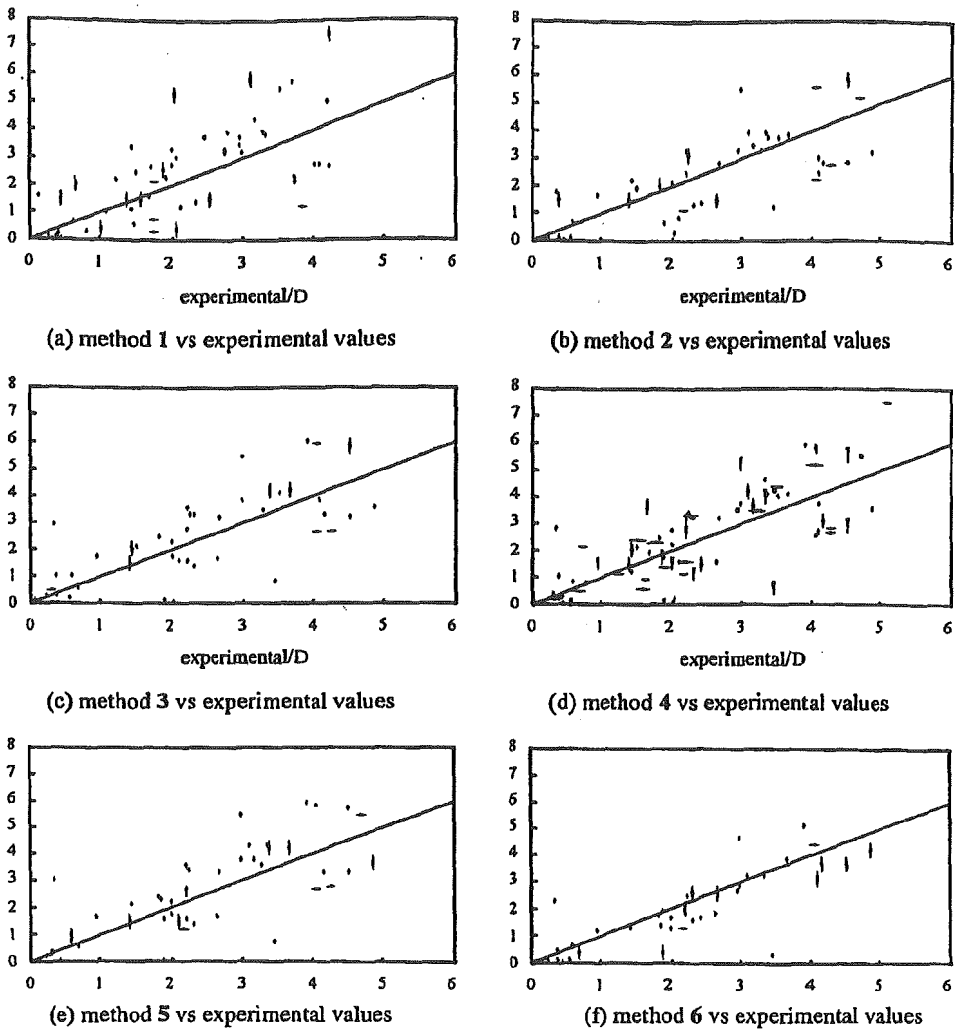


Fig. 3. Correlation between calculated and experimental dipole moments. The experimental dipole moments are taken in a horizontal axis and the those calculated by QEq methods are taken in the vertical axis.

dipole moments. RMSDs and correlation coefficients relating the calculated and experimental values were evaluated. The results for sets **i** and **ii** are shown in Table 7, and those for sets **iii** and **iv** in Table 8. The dipole moments evaluated from HF-ESP charges are closest to the experimental values. Method **6** gave the next closest results, whereas the other QEq methods were much less successful in

Table 7
RMSD and correlation between calculational and experimental dipole moments

| | 1 | 2 | 3 | 4 | 5 | 6 | QEq | G–H |
|---|---|---|---|---|---|---|---|---|
| Set i | | | | | | | | |
| RMSD | 1.125 | 1.158 | 1.254 | 1.228 | 1.244 | 0.821 | 1.113 | 0.992 |
| Correlation | 0.721 | 0.722 | 0.723 | 0.723 | 0.724 | 0.815 | 0.692 | 0.719 |
| Set ii | | | | | | | | |
| RMSD | 0.928 | 0.950 | 1.023 | 0.995 | 1.000 | 0.524 | 0.942 | 0.805 |
| correlation | 0.754 | 0.757 | 0.780 | 0.780 | 0.787 | 0.909 | 0.734 | 0.844 |

The Gasteiger–Hückel charges are calculated for compounds except for carbon monoxide in (a). Abbreviation is the same as Table 4.

Table 8
RMSD and correlation between calculational and experimental dipole moments for compounds sets without Bakowies et al. test sets

| | 1 | 2 | 3 | 4 | 5 | 6 | QEq | G–H |
|---|---|---|---|---|---|---|---|---|
| Set iii | | | | | | | | |
| RMSD | 1.188 | 1.224 | 1.291 | 1.263 | 1.283 | 0.852 | 1.156 | 1.067 |
| correlation | 0.731 | 0.732 | 0.743 | 0.744 | 0.745 | 0.829 | 0.714 | 0.713 |
| Set iv | | | | | | | | |
| RMSD | 0.978 | 1.010 | 1.079 | 1.045 | 1.062 | 0.553 | 0.991 | 0.865 |
| correlation | 0.771 | 0.773 | 0.792 | 0.794 | 0.799 | 0.915 | 0.754 | 0.860 |

Abbreviation is the same as Table 4.

Table 9
Atomic charges on α- and β-D-idose

| | 1 | 2 | 3 | 4 | 5 | 6 | HF-ESP |
|---|---|---|---|---|---|---|---|
| α-D-Idose | | | | | | | |
| C-1 | 0.173 | 0.202 | 0.687 | 0.628 | 0.726 | 0.502 | 0.535 |
| C-2 | 0.085 | 0.095 | 0.147 | 0.137 | 0.076 | 0.096 | −0.116 |
| C-3 | 0.076 | 0.087 | 0.232 | 0.216 | 0.230 | 0.159 | 0.285 |
| C-4 | 0.072 | 0.081 | 0.205 | 0.192 | 0.167 | 0.146 | −0.034 |
| C-5 | 0.082 | 0.093 | 0.187 | 0.165 | 0.183 | 0.133 | 0.015 |
| C-6 | 0.045 | 0.050 | 0.162 | 0.144 | 0.144 | 0.113 | 0.237 |
| H-7 | 0.145 | 0.154 | 0.051 | 0.076 | 0.053 | 0.040 | 0.058 |
| H-8 | 0.121 | 0.127 | 0.102 | 0.113 | 0.125 | 0.073 | 0.135 |
| H-9 | 0.125 | 0.134 | 0.126 | 0.136 | 0.138 | 0.092 | 0.102 |
| H-10 | 0.102 | 0.105 | 0.063 | 0.073 | 0.077 | 0.045 | 0.128 |
| H-11 | 0.131 | 0.140 | 0.107 | 0.121 | 0.121 | 0.080 | 0.103 |
| H-12 | 0.109 | 0.114 | 0.115 | 0.121 | 0.116 | 0.083 | 0.073 |
| H-13 | 0.133 | 0.143 | 0.139 | 0.146 | 0.153 | 0.101 | 0.034 |
| O-14 | −0.440 | −0.489 | −0.954 | −0.939 | −0.886 | −0.708 | −0.695 |
| O-15 | −0.462 | −0.514 | −0.941 | −0.932 | −0.854 | −0.692 | −0.633 |
| O-16 | −0.476 | −0.531 | −0.990 | −0.981 | −0.910 | −0.722 | −0.722 |
| O-17 | −0.455 | −0.506 | −0.912 | −0.907 | −0.832 | −0.680 | −0.624 |
| O-18 | −0.388 | −0.425 | −0.709 | −0.682 | −0.715 | −0.529 | −0.442 |
| O-19 | −0.448 | −0.496 | −0.862 | −0.859 | −0.794 | −0.650 | −0.689 |
| H-20 | 0.271 | 0.307 | 0.669 | 0.668 | 0.583 | 0.512 | 0.464 |
| H-21 | 0.231 | 0.257 | 0.525 | 0.521 | 0.459 | 0.394 | 0.444 |
| H-22 | 0.220 | 0.246 | 0.530 | 0.525 | 0.459 | 0.396 | 0.447 |
| H-23 | 0.280 | 0.319 | 0.691 | 0.691 | 0.613 | 0.532 | 0.453 |
| H-24 | 0.271 | 0.307 | 0.630 | 0.627 | 0.566 | 0.484 | 0.443 |
| *β-D-Idose* | | | | | | | |
| C-1 | 0.169 | 0.197 | 0.675 | 0.613 | 0.706 | 0.489 | 0.314 |
| C-2 | 0.089 | 0.101 | 0.197 | 0.186 | 0.129 | 0.135 | 0.260 |
| C-3 | 0.070 | 0.080 | 0.194 | 0.178 | 0.178 | 0.133 | −0.072 |
| C-4 | 0.079 | 0.090 | 0.240 | 0.226 | 0.218 | 0.172 | 0.356 |
| C-5 | 0.080 | 0.091 | 0.194 | 0.168 | 0.178 | 0.138 | −0.107 |
| C-6 | 0.046 | 0.051 | 0.159 | 0.142 | 0.149 | 0.111 | 0.284 |
| H-7 | 0.124 | 0.130 | 0.006 | 0.035 | 0.009 | 0.010 | 0.066 |
| H-8 | 0.113 | 0.117 | 0.065 | 0.077 | 0.090 | 0.046 | 0.060 |

Table 9 (*continued*)

| | 1 | 2 | 3 | 4 | 5 | 6 | HF-ESP |
|---|---|---|---|---|---|---|---|
| H-9 | 0.123 | 0.131 | 0.116 | 0.126 | 0.133 | 0.084 | 0.152 |
| H-10 | 0.115 | 0.122 | 0.122 | 0.132 | 0.125 | 0.091 | 0.099 |
| H-11 | 0.113 | 0.118 | 0.077 | 0.091 | 0.089 | 0.059 | 0.120 |
| H-12 | 0.093 | 0.095 | 0.038 | 0.046 | 0.049 | 0.024 | −0.016 |
| H-13 | 0.152 | 0.167 | 0.212 | 0.219 | 0.218 | 0.157 | 0.093 |
| O-14 | −0.445 | −0.496 | −0.990 | −0.971 | −0.914 | −0.725 | −0.706 |
| O-15 | −0.449 | −0.501 | −0.955 | −0.947 | −0.857 | −0.705 | −0.721 |
| O-16 | −0.478 | −0.531 | −0.926 | −0.918 | −0.865 | −0.680 | −0.721 |
| O-17 | −0.453 | −0.504 | −0.923 | −0.917 | −0.844 | −0.687 | −0.749 |
| O-18 | −0.378 | −0.413 | −0.681 | −0.652 | −0.683 | −0.509 | −0.365 |
| O-19 | −0.443 | −0.489 | −0.821 | −0.817 | −0.760 | −0.620 | −0.684 |
| H-20 | 0.267 | 0.301 | 0.614 | 0.609 | 0.543 | 0.462 | 0.474 |
| H-21 | 0.275 | 0.312 | 0.654 | 0.652 | 0.577 | 0.494 | 0.485 |
| H-22 | 0.221 | 0.246 | 0.522 | 0.518 | 0.460 | 0.393 | 0.468 |
| H-23 | 0.284 | 0.323 | 0.688 | 0.689 | 0.610 | 0.529 | 0.485 |
| H-24 | 0.233 | 0.261 | 0.520 | 0.517 | 0.463 | 0.399 | 0.422 |

reproducing the experimental results. This tendency was apparent whether or not the compound set included the reference molecules used for BT parameterization. Dipole moments calculated by QEq methods other than method 6 were less appropriate than those derived from Gasteiger–Hückel charges, which are not geometry-dependent. These results suggest that BT parameters are

Table 10
Difference between the atomic charges of α-and β-D-idose

| | 1 | 2 | 3 | 4 | 5 | 6 | HF-ESP |
|---|---|---|---|---|---|---|---|
| C-1 | −0.004 | −0.005 | −0.012 | −0.015 | −0.019 | −0.013 | −0.221 |
| C-2 | 0.004 | 0.005 | 0.051 | 0.048 | 0.053 | 0.039 | 0.376 |
| C-3 | −0.006 | −0.007 | −0.038 | −0.038 | −0.052 | −0.026 | −0.357 |
| C-4 | 0.007 | 0.009 | 0.035 | 0.035 | 0.050 | 0.026 | 0.390 |
| C-5 | −0.002 | −0.002 | 0.007 | 0.004 | −0.005 | 0.005 | −0.122 |
| C-6 | 0.001 | 0.002 | −0.003 | −0.003 | 0.005 | −0.002 | 0.048 |
| H-7 | −0.021 | −0.024 | −0.045 | −0.042 | −0.045 | −0.030 | 0.008 |
| H-8 | −0.008 | −0.010 | −0.037 | −0.035 | −0.036 | −0.027 | −0.075 |
| H-9 | −0.002 | −0.003 | −0.010 | −0.010 | −0.005 | −0.008 | 0.050 |
| H-10 | 0.013 | 0.017 | 0.059 | 0.059 | 0.048 | 0.045 | −0.029 |
| H-11 | −0.018 | −0.022 | −0.030 | −0.030 | −0.032 | −0.021 | 0.017 |
| H-12 | −0.015 | −0.019 | −0.076 | −0.076 | −0.068 | −0.059 | −0.090 |
| H-13 | 0.019 | 0.024 | 0.072 | 0.073 | 0.065 | 0.057 | 0.059 |
| O-14 | −0.004 | −0.006 | −0.035 | −0.032 | −0.028 | −0.018 | −0.011 |
| O-15 | 0.012 | 0.014 | −0.015 | −0.014 | −0.003 | −0.013 | −0.089 |
| O-16 | −0.001 | 0.000 | 0.065 | 0.063 | 0.046 | 0.042 | 0.001 |
| O-17 | 0.002 | 0.002 | −0.011 | −0.010 | −0.013 | −0.007 | −0.124 |
| O-18 | 0.010 | 0.013 | 0.028 | 0.031 | 0.033 | 0.020 | 0.077 |
| O-19 | 0.004 | 0.007 | 0.042 | 0.042 | 0.034 | 0.030 | 0.005 |
| H-20 | −0.004 | −0.006 | −0.054 | −0.059 | −0.040 | −0.050 | 0.011 |
| H-21 | 0.045 | 0.055 | 0.129 | 0.131 | 0.118 | 0.100 | 0.041 |
| H-22 | 0.000 | 0.001 | −0.008 | −0.007 | 0.001 | −0.002 | 0.021 |
| H-23 | 0.004 | 0.004 | −0.003 | −0.003 | −0.003 | −0.003 | 0.033 |
| H-24 | −0.038 | −0.046 | −0.111 | −0.110 | −0.103 | −0.085 | −0.021 |

desirable for accurate calculations of dipole moments and, in contrast to atomic charge calculations, that the parameterization of $J_{II}$ and $\chi_I^0$ plays a more important role in dipole moment calculations than the type of empirical approximation of $J_{IJ}$.

In order to test the effectiveness of the QEq methods in more complicated calculations, atomic charges of α- and β-D-idose (which has been discussed in Ref. [5]) were evaluated (Table 9). The differences between the atomic charges of α- and β-D-idose calculated using the six methods are shown in Table 10. As is evident in Table 9, it was found that all methods qualitatively reproduced the HF-ESP results, method **6** in particular giving the most reasonable values for both α- and β-D-idose. With respect to the differences in charges, methods **3**–**5** reproduced the HF-ESP results equally as well as method **6** (for example, compare the negative differences of O-14, O-15 and O-17 with the positive values of O-16, O-18 and O-19). These results suggest that the six types of QEq methods can also be classified in two groups with respect to their success in calculating the atomic charges for various molecular topologies: the less successful group consists of methods **1** and **2** while the more successful group consists of methods **3**–**6**. The types of approximations for $J_{IJ}$ may play a more important role in atomic charge calculations of enantiomers than the parameterization of $J_{II}$ and $\chi_I^0$.

## 4. Conclusion

In this study, the atomic charges and dipole moments of various molecules were calculated by QEq methods using five types of empirical approximation for $J_{IJ}$, and then assessed relative to one another. We found that methods **5** and **6** were appropriate for $J_{IJ}$ calculations of the QEq method. Since both methods are undemanding in terms of computational resources, easy calculation of atomic charges at every step of MM and MD calculations are expected. For the DasGupta–Huzinaga approximation, only RG parameters were used in this study; it is possible that even better results may be obtained by using specific parameters for this approximation similar to the BT parameters specified for the Ohno–Klopman equation. Furthermore, on introducing more explicit types of atom (imitating atom types of the MM method) such as 'nitrogen in nitro group' and parameterizing for each atom type, the QEq method is expected to allow the accurate calculation of atomic charges and dipole moments even for compounds whose atomic charges could not be evaluated in this study. We intend to investigate these aspects in a future study.

## References

[1] U.C. Singh, P.A. Kollman, J. Comput. Chem. 5 (1984) 129.
[2] J. Gasteiger, M. Marsili, Tetrahedron 36 (1980) 3219.
[3] K.-H. Cho, Y.K. Kang, K.T. No, H.A. Sheraga, J. Phys. Chem. 105 (2001) 3624.
[4] A.K. Rappé, W.A. Goddard III, J. Phys. Chem. 95 (1991) 3358.
[5] D. Bakowies, W. Thiel, J. Comput. Chem. 17 (1996) 87.
[6] T. Nakano, T. Kaminuma, M. Uebayasi, Y. Nakata, Chem-Bio Inf. J. 1 (2001) 35.
[7] K. Ohno, Theor. Chim. Acta (Berl.) 2 (1964) 219.
[8] G. Klopman, J. Am. Chem. Soc. 87 (1965) 3300.
[9] K. Nishimoto, N. Mataga, Z. Phys. Chem. 13 (1957) 140.
[10] J. Ridley, M. Zerner, Theor. Chim. Acta (Berl.) 32 (1973) 111.
[11] A. DasGupta, S. Huzinaga, Theor. Chim. Acta (Berl.) 35 (1974) 329.
[12] R.S. Mulliken, J. Chem. Phys. 2 (1934) 782.
[13] ArgusLab 3.0, Planaria Software, Seattle, 2002.
[14] The Chemical Society of Japan (Eds.), Kagaku Binran, fourth ed., Maruzen, Tokyo, 1993, p. II-575.
[15] M. Allegrini, J.W.C. Johns, A.R.W. McKellar, J. Chem. Phys. 70 (1979) 2829.
[16] K.M. Merz, J. Comput. Chem. 13 (1992) 749.
[17] M.W. Schmidt, K.K. Baldridge, J.A. Boatz, S.T. Elbert, M.S. Gordon, J.H. Jensen, S. Koseki, N. Matsunaga, K.A. Nguyen, S.J. Su, T.L. Windus, M. Dupuis, J.A. Montgomery, J. Comput. Chem. 14 (1993) 1347.
[18] SYBYL 6.8, Tripos Inc., St Louis, 2001.

Environmental and Molecular Mutagenesis 42:288–298 (2003)

# Deletion, Rearrangement, and Gene Conversion; Genetic Consequences of Chromosomal Double-Strand Breaks in Human Cells

Masamitsu Honma,[1]* Masako Izumi,[2] Mayumi Sakuraba,[1] Satoshi Tadokoro,[1] Hiroko Sakamoto,[1] Wensheng Wang,[1] Fumio Yatagai,[2] and Makoto Hayashi[1]

[1]*Division of Genetics and Mutagenesis, National Institute of Health Sciences, Setagaya, Tokyo*

[2]*Division of Radioisotope Technology, Institute of Physical and Chemical Research, Wako, Saitama, Japan*

Chromosomal double-strand breaks (DSBs) in mammalian cells are usually repaired through either of two pathways: end-joining (EJ) or homologous recombination (HR). To clarify the relative contribution of each pathway and the ensuing genetic changes, we developed a system to trace the fate of DSBs that occur in an endogenous single-copy human gene. Lymphoblastoid cell lines TSCE5 and TSCER2 are heterozygous (+/−) or compound heterozygous (−/−), respectively, for the thymidine kinase gene (*TK*), and we introduced an I-*Sce*I endonuclease site into the gene. EJ for a DSB at the I-*Sce*I site results in TK-deficient mutants in TSCE5 cells, while HR between the alleles produces TK-proficient revertants in TSCER2 cells. We found that almost all DSBs were repaired by EJ and that HR rarely contributes to the repair in this system. EJ contributed to the repair of DSBs 270 times more frequently than HR. Molecular analysis of the *TK* gene showed that EJ mainly causes small deletions limited to the *TK* gene. Seventy percent of the small deletion mutants analyzed showed 100- to 4,000-bp deletions with a 0- to 6-bp homology at the joint. Another 30%, however, were accompanied by complicated DNA rearrangements, presumably the result of sister-chromatid fusion. HR, on the other hand, always resulted in non-crossing-over gene conversion without any loss of genetic information. Thus, although HR is important to the maintenance of genomic stability in DNA containing DSBs, almost all chromosomal DSBs in human cells are repaired by EJ. Environ. Mol. Mutagen. 42:288–298, 2003. 

**Key words: double-strand breaks; end-joining; inter-allelic recombination; human somatic cells.**

## INTRODUCTION

Chromosomal double-strand breaks (DSBs), either arising spontaneously or induced by ionizing radiation, are particularly dangerous lesions, and their repair is important for maintaining the genomic integrity of all organisms [Van Dyck et al., 1999]. The failure to repair DSBs or their inaccurate repair may be mutagenic or lethal to cells, and can cause genetic defects that lead to genetic diseases and cancers [Khanna and Jackson, 2001; van Gent et al., 2001]. DSBs are usually repaired through either end-joining (EJ) or homologous recombination (HR) [Haber, 2000; Jackson, 2002]. EJ joins sequences at the broken ends with little or no homology in a nonconservative manner and, as a result, some genetic information is lost. HR, in contrast, requires extensive tracts of sequence homology and is basically a conservative repair pathway. HR can occur by gene conversion with or without crossing-over [Giver and Grosovsky, 1997; Cromie et al., 2001]. Non-crossing-over only involves the localized DNA region surrounding the DSB, whereas crossing-over results in a switch of the linkage relationships of all alleles from the break point to the telomere. The repair of DSBs has been studied extensively in the yeast *Saccharomyces cerevisiae* [Paques and Haber, 1999]. HR is the primary pathway for repairing DSBs in yeast and almost always results in gene conversion without crossing-over [Haber, 1995]. This is in striking contrast to mammalian cells, where EJ is thought to be the predominant mechanism for repairing DSBs [Jackson and Jeggo, 1995]. However, the relative contribution of the two pathways and

Grant sponsor: Nuclear Energy Research Grants from the Ministry of Education, Culture, Sports, Science, and Technology of Japan.

*Correspondence to: Masamitsu Honma, Division of Genetics and Mutagenesis, National Institute of Health Sciences, 1-18-1 Kamiyoga, Setagaya-ku, Tokyo 158-8501, Japan. E-mail: honma@nihs.go.jp

Received 19 May 2003; provisionally accepted 9 August 2003; and in final form 22 August 2003

DOI 10.1002/em.10201

Published online 8 December 2003 in Wiley InterScience (www.interscience.wiley.com).

their interaction in mammalian cells has not been firmly established.

In the study of DSB repair in mammalian cells, we employed the TK6 human lymphoblastoid cell line that is heterozygous for the thymidine kinase (*TK*) gene on chromosome 17q [Honma et al., 1997a,b, 2000]. The *TK*-gene mutation assay using the TK6 cells was first developed by Liber and Thilly [1982]. It can detect not only intragenic point mutations, but also loss of the functional allele (loss of heterozygosity [LOH]), which is considered a consequence of the repair of chromosomal DSBs. For repair of a DSB in the functional *TK* allele, HR produces homozygosity of the nonfunctional *TK* allele, while EJ brings about deletion in the functional *TK* allele, leading to its hemizygosity [Honma et al., 1997b]. We have demonstrated that homozygous LOH is the predominant spontaneous event, whereas hemizygous LOH is induced by ionizing irradiation, implying that HR repairs infrequently occurring DSBs, maintaining genomic integrity, whereas EJ repairs extensive DNA damage, enabling cell survival [Honma et al., 1997a; Jackson, 2002]. The mutational spectrum in the *TK* gene induced by nontargeting mutagenesis, however, has a strong bias for the recovery of HR mutants with crossing-over [Quintana et al., 2001]. DSBs generated within the *TK* gene can be recovered by any repair pathway as TK-deficient mutants. HR mutants with crossing-over, however, frequently result from the repair of DSBs outside the *TK* gene, which cannot be recovered by EJ and HR without crossing-over, because such genetic events are localized and do not affect the *TK* gene. Thus, the mutational spectrum for nontargeted mutagenesis does not provide appropriate information to elucidate the relative contribution of each DSB repair pathway.

Recently, an understanding of mammalian EJ and HR has emerged from systems that use the rare cutting restriction endonuclease I-*Sce*I from *Saccharomyces cerevisiae* [Johnson and Jasin, 2001]. Because the 18-bp recognition sequence of I-*Sce*I is infrequent enough to be naturally absent from most genomes, and can be introduced into a chromosome by transfection, it is possible to generate site-specific DSBs in a mammalian chromosome by expressing the enzyme in the genetically modified cells. Using this unique system, it has been demonstrated that DSBs in mammalian chromosomes initiate HR as well as EJ, and that deficiency or overexpression of *Rad51* and its paralogues, which have a central role in HR, can influence the efficiency of HR [Rijkers et al., 1998; Cui et al., 1999; Takata et al., 2001]. These systems, however, have used artificial reporter substrates based on exogenous drug-resistance genes and are biased in favor of detecting specific deletion and recombination events [Taghian and Nickoloff, 1997; Sargent et al., 1997; Liang et al., 1998; Lin et al., 1999]. Most of these models, in particular, cannot detect inter-allelic recombination, which is expected to be a major HR pathway for repairing chromosomal DSBs in mammalian cells. Moynahan and Jasin [1997] engineered a recombinational substrate containing an I-*Sce*I site integrated into the retinoblastoma (*Rb*) gene of mouse embryonic stem cells and demonstrated a significant contribution of inter-allelic recombination for repairing DSBs, but the contribution of EJ was not clear. Thus, the previous DSB studies using the I-*Sce*I system have been useful for elucidating the molecular mechanisms of the repair pathways, but do not provide a general model for demonstrating the fate of a DSB in mammalian cells.

In the present study, we developed a system to trace the fate of DSBs that occur in a single-copy human gene. We introduced an I-*Sce*I site into the endogenous *TK* gene of TK6 cells by gene targeting. Unlike nontargeted mutagenesis, this system makes it possible to recover efficiently cell clones resulting from the repair of DSBs at a defined site. Using this system, we evaluated the relative contribution of EJ and HR for repairing DSBs and investigated the genetic consequences of each pathway at the molecular and cytogenetic level. This is the first report tracing the fate of a DSB occurring in an endogenous single-copy gene in the human genome.

## MATERIALS AND METHODS

### Vectors

The first targeting vector, pTK4, was designed to disrupt exon 5 of the *TK* gene by replacement with a *neo* gene. It was constructed as follows: (1) a region containing exons 6 and 7 of the *TK* gene (position 12,002–13,367) was amplified by a polymerase chain reaction (PCR) in which a *Xba*I linker was added to the 5′-primer. The amplified product was cleaved by *Xba*I and *Bam*HI and was cloned into pBluescript II (Stratagene, La Jolla, CA); (2) a 1,637-bp *Ssp*I-*Eco*O109I DNA fragment containing a simian virus 40 (SV-40) early-promoter-driven *neo* gene was cleaved from pEGFP-C1 (BD Biosciences-Clontech, Tokyo, Japan), modified with a *Not*I linker, and then cloned into the above plasmid; and (3) a region containing the last part of intron 4 (position 9,291–11,850) was amplified using a 3′-primer modified with a *Sac*II linker. The PCR product was cleaved by *Sac*I and *Sac*II, and cloned into the above plasmid.

The second targeting vector, pTK10, consisted of about 6 kb of the original *TK* gene encompassing exons 5, 6, and 7, and an I-*Sce*I site, which was used to revert the *TK* gene disrupted by pTK4. To construct pTK10, a region containing exons 5, 6, and 7 (positions 7,248–13,367) was amplified using a 5′-primer modified with a *Xho*I linker. The PCR product was cleaved by *Xho*I and *Bam*HI, and cloned into pBluescript II. A 31-bp DNA fragment containing the 18-bp I-*Sce*I site was formed by annealing the two oligonucleotides (5′-gatccATTACCCTGTTATCCCTActctcgag-3′ and 5′-gatctcgagagTAGGGATAACAGGGTAATg-3′), producing *Bgl*II compatible sites at both ends. The DNA fragment was inserted into the *Bgl*II site of the above plasmid.

The I-*Sce*I-expressing vector, pCMV3xnls-I-*Sce*I (kindly provided by Dr. J. Nickoloff, University of New Mexico School of Medicine, Albuquerque, NM), contains the I-*Sce*I-nuclease coding sequence fused at its 5′-end to a triplicate nuclear localization signal, driven by the CMV promoter, and terminated by the bovine growth hormone polyadenylation signal [Brenneman et al., 2002].

### Cell Construction

TK6 human lymphoblastoid cells are heterozygous for a point mutation in exon 4 of the *TK* gene [Grosovsky et al., 1993]. They were grown in

RPMI 1640 medium (Gibco-Invitrogen, Carlsbad, CA), supplemented with 10% heat-inactivated horse serum (JRH Biosciences, Lenexa, KS). TK-deficient clones were generated by transfecting cells with the first targeting vector that had been linearized with *Sca*I. TK6 cells ($2 \times 10^7$) were suspended with 20 μg of the linearized vector DNA in 0.8 ml of serum-free RPMI 1640 medium, transferred into a 0.4-cm gap chamber, and electroporated with an electroporation unit (Bio-Rad, Hercules, CA) set at 950 μF and 250 V. After 72 hr, the cells were seeded into 96-well microwell plates in the presence of 2.0 μg/ml trifluorothymidine (TFT) and 500 μg/ml G418. TK-deficient clones were isolated 2 weeks later, as described previously [Honma et al., 1997a]. One of clones, TKp4-2, was found to have the desired disruption of the *TK* gene (Fig. 1a). To obtain TK-revertant clones with an I-*Sce*I site in the *TK* gene, we transfected TKp4-2 cells ($2 \times 10^7$) with the linearized second targeting vector, using the same techniques used above, and isolated histone acetyltransferase (HAT) (200 μM hypoxanthine, 0.1 μM aminopterin, 17.5 μM thymidine)-resistant clones. One revertant clone, TSCE5, was identified and its molecular structure was confirmed by PCR analysis (Fig. 1a). The cell line TSCER2 was spontaneously generated as a TK-deficient clone from TSCE5. It had a point mutation (G→A transition) at the bp 23 of exon 5 in the *TK* allele containing the I-*Sce*I site, resulting in a compound heterozygote ($TK^{-/-}$) (Fig. 1a).

### I-SceI Expression

A total of $1 \times 10^7$ cells were transfected in serum-free RPMI 1640 medium by electroporation with 20 μg of uncut pCMV3xnls-I-*Sce*I vector or without vector as a control. After 72 hr, the cells were seeded into 96-well microwell plates in the presence of TFT (for TSCE5) or HAT (for TSCER2). Drug-resistant colonies were counted 2 weeks later and independently expanded.

### DNA and Cytogenetic Analysis

DNA extraction and PCR analysis for LOH analysis at polymorphic sites in the *TK* gene and microsatellite markers were performed as described [Honma et al., 2000]. PCR analyses at the I-*Sce*I site were performed to amplify the following products with the specified primers: the short fragment (Fig. 1a,b), 164F (5′-TGGGAGAATTAAGAGTTACTCC-3′) and 196R (5′-AGC TTCCACCCCAGCAGCAGCT-3′); and the long fragment (see Fig. 4a,b), 175F (5′-TCGCTTGGCAATAGTAGGAGCT-3′) and 199R (5′-ACTCTGTCTGTGCCGAGTGTA-3′). Amplification was performed by denaturation at 94°C for 5 min, followed by 25 cycles of 94°C for 1 min, 57°C for 1 min, 72°C for 2 min, and extension at 72°C for 10 min. PCR products were analyzed using an Agilent 2100 Bioanalyzer (Agilent Technologies, Waldbronn, Germany) and sequenced with an ABI 310 genetic analyzer (Applied Biosystems, Foster City, CA).

Spectral karyotyping (SKY) was used for the cytogenetic analysis of some TK-deficient mutants. The procedure was performed according to the manufacturer's recommendations as previously described [Honma et al., 2002]. Metaphase images were captured and analyzed on a SKY vision cytogenetics workstation (Applied Spectral Imaging, Carlsbad, CA) attached to an Olympus model 50 fluorescence microscope. At least five metaphase cells were analyzed per slide.

## RESULTS

### Experimental Design

To investigate the fate of DSBs occurring in the human genome, we used human lymphoblastoid cells containing an I-*Sce*I recognition site in the endogenous *TK* gene. Human lymphoblastoid TK6 cells are heterozygous ($TK^{+/-}$) for a point mutation in exon 4 of the *TK* gene, which is on chromosome 17q. We introduced an I-*Sce*I sequence into intron 4 near exon 5 of the functional *TK* allele. We employed two steps for gene targeting to minimize sequence divergence between the alleles (Fig. 1a), because integrated exogenous DNA sequences reduce sequence homology between alleles and probably suppresses inter-allelic recombination [Elliott et al., 1998]. The functional *TK* allele was first disrupted by replacement with a *neo* gene, and then it was reverted by a second targeting vector, pTK10, consisting of 6 kb of the original *TK* gene including exons 5, 6, and 7 and containing an I-*Sce*I site. One of the recombinants, TSCE5, had a 31-bp DNA fragment containing the 18-bp I-*Sce*I site inserted 75 bp upstream of exon 5 (Fig. 1b). TSCE5 cells can grow in HAT medium, but not in TFT medium (HAT-resistant/TFT-sensitive; $HAT^r/TFT^s$). We next isolated spontaneously generated TK-deficient mutants from TSCE5. One of the mutants, TSCER2, had a point mutation (G→A transition) at bp 23 of exon 5. TSCER2 is compound heterozygote ($TK^{-/-}$) for the *TK* gene and is $HAT^s/TFT^r$.

Figure 1c shows the strategy used for detecting EJ in TSCE5 cells and HR in TSCER2 cells. When a DSB at the I-*Sce*I site is repaired by EJ, a TK-deficient deletion mutant is isolated as $TFT^r$ in TSCE5 cells. With HR repair, on the other hand, a TK-proficient revertant, which is generated by inter-allelic recombination, is selected by HAT in TSCER2 cells. Theoretically, TSCE5 cells can also detect HR, if HR with crossing-over or long tract gene conversion makes the point mutation in exon 4 homozygous ($TK^{-/-}$). We can, however, distinguish these events by further molecular analysis. Because both cell lines are identical except for their *TK* status and because the DSB occurs at the same position in both cell lines, this system can evaluate the contribution of EJ and HR without bias when the experiments are conducted simultaneously in both cell lines using the same conditions.

### Almost All Chromosomal DSBs Were Repaired by EJ, But Not by HR

We transfected an I-*Sce*I expression vector, pCMV3xnls-I-*Sce*I, into TSCE5 cells by electroporation. TK-deficient mutant cells appeared at an average frequency of $274 \times 10^{-6}$, more than 130-fold higher than in nontransfected cells (Fig. 2a). Because the transfection of the expression vector did not affect the mutant frequencies for the *HPRT* gene in TSCE5 cells and the *TK* gene in the original TK6 cells, the increase in mutant frequency must have been due to repair of DSBs at the I-*Sce*I site (Fig. 2a). When TSCER2 cells were transfected with the I-*Sce*I expression vector under the same conditions, TK-proficient revertants were isolated at an average frequency of $1.07 \times 10^{-6}$, more than 200-fold higher than spontaneously occurring events (Fig. 2b). This strongly suggests that inter-allelic HR is also

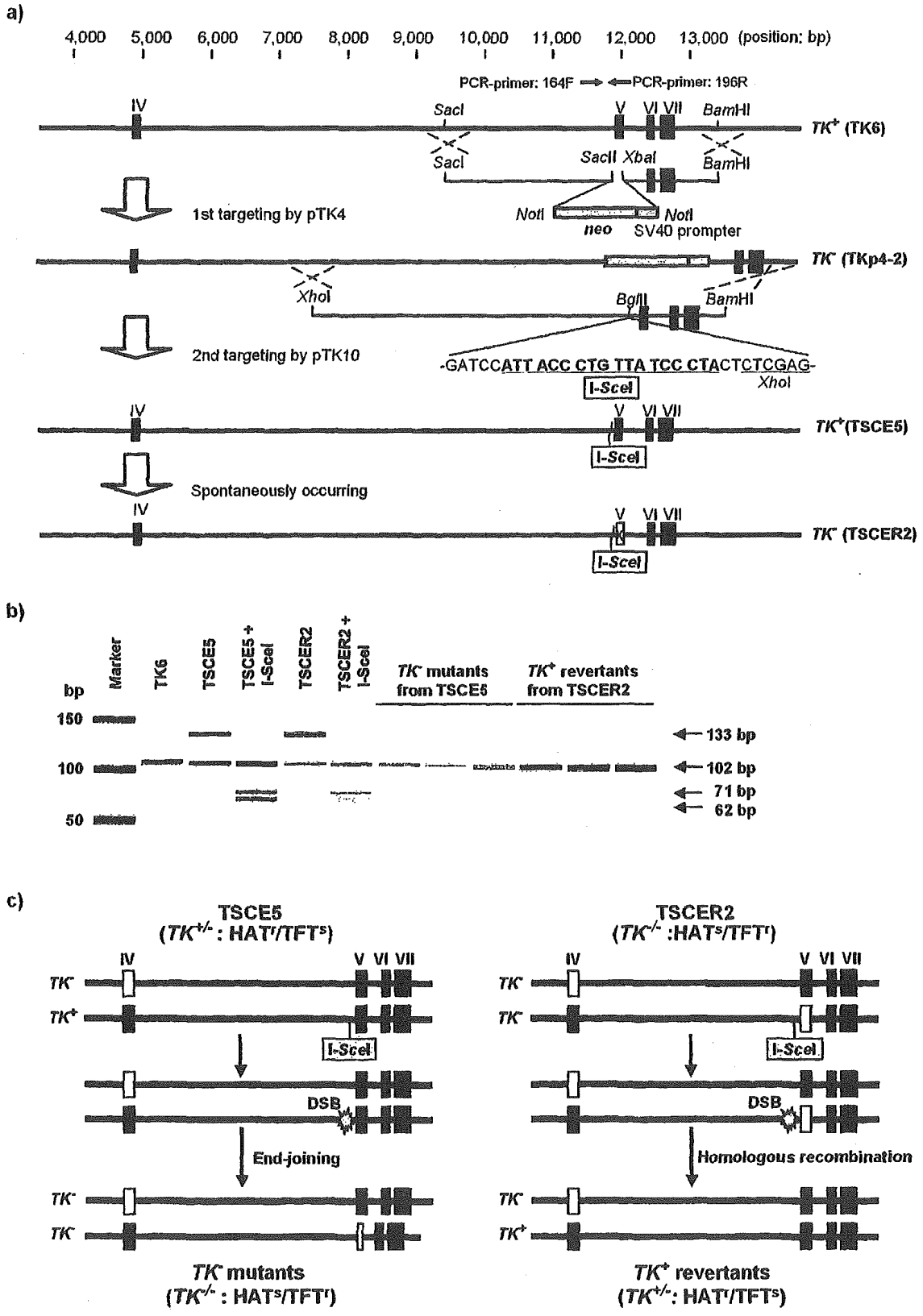
a)
4,000 5,000 6,000 7,000 8,000 9,000 10,000 11,000 12,000 13,000 (position: bp)
PCR-primer: 164F
PCR-primer: 196R
IV
SacI
V VI VII
BamHI
TK+ (TK6)
SacI
SacII XbaI
BamHI
1st targeting by pTK4
NotI
neo
NotI
SV40 prompter
TK- (TKp4-2)
XhoI
BglII
BamHI
2nd targeting by pTK10
-GATCCATT ACC CTG TTA TCC CTACTCTCGAG-
I-SceI
XhoI
TK+(TSCE5)
Spontaneously occurring
TK- (TSCER2)
b)
bp
Marker
TK6
TSCE5
TSCE5 + I-SceI
TSCER2
TSCER2 + I-SceI
TK- mutants from TSCE5
TK+ revertants from TSCER2
150
100
50
133 bp
102 bp
71 bp
62 bp
c)
TSCE5
(TK+/- : HATr/TFTs)
TSCER2
(TK-/- :HATs/TFTr)
TK-
TK+
I-SceI
DSB
End-joining
Homologous recombination
TK- mutants
(TK-/- : HATs/TFTr)
TK+ revertants
(TK+/-: HATr/TFTs)

Figure 1.

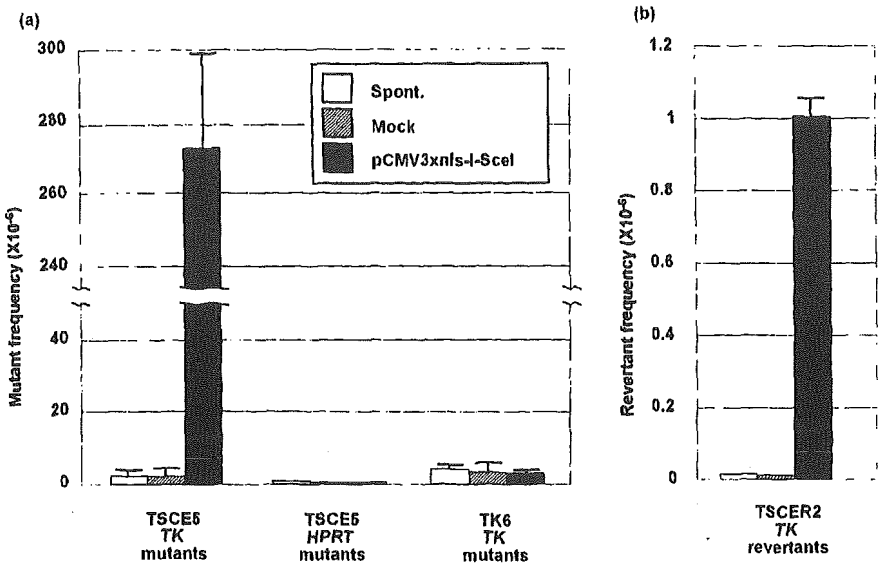


**Fig. 2.** Double-strand breaks (DSBs) induce both end-joining (EJ) and homologous recombination (HR). **a:** Transfection of TSCE5 cells with the I-*Sce*I expression vector increases the thymidine kinase (TK)-deficient mutant frequency more than 130-fold compared with the control. No transfection-induced mutant induction was observed for the *HPRT* gene in TSCE5 cells and the *TK* locus in TK6 cells. **b:** Transfection of TSCER2 cells also increases the TK-proficient revertant frequency more than 200-fold compared with the control.

induced by a DSB. However, the fraction of HR was estimated to be much less than that of EJ, indicating that almost all DSBs were repaired by EJ.

## EJ Mainly Caused Simple Deletions, But Also Produced Complicated DNA Rearrangements

We examined 44 TK-deficient mutants from TSCE5 cells at the molecular level. Every mutant lost the I-*Sce*I site (Fig. 1b) by deletion and were hemizygous for the nonfunctional allele, suggesting that every mutant was generated by EJ. To obtain a rough determination of the extent of the deletion, we analyzed LOH at polymorphic sites within the *TK* gene and at 5 polymorphic microsatellite loci surrounding the *TK* gene. The 13.5-kb human *TK* gene is located on chromosome 17q23.2. The *TK* gene in TSCE5 and TSCER2 cells has frame-shift dimorphisms in exons 4 and exon 7, which are 6,950 and 876 bp, respectively, from the I-*Sce*I site. The 1-bp difference in the PCR products from these regions facilitated the LOH analysis [Honma et al., 2000]. Eleven (25%) of the mutants had small deletions not extending to either poymorphic site, and 26 (59%) showed medium-size deletions involving only the exon 4 and/or 7 polymorphic site in the *TK* gene. The remaining 7 mutants (16%) were the result of large interstitial or terminal deletions (Fig. 3).

We further analyzed small and medium deletions by PCR and direct sequencing to determine the exact size of deletions and the junction sequences generated by EJ. Eleven small and 23 medium deletion I mutants identified by LOH analysis were subjected to PCR using primers 175F and 199R, which amplified 5,618 bp (I-*Sce*I allele) and 5,587 bp (non-I-*Sce*I allele) products using DNA from TSCE5 cells (Fig. 4a,b). Twenty-two of the 34 mutants exhibited shorter PCR products of various sizes in addition to the original product in the gel analysis, whereas the other 12 mutants did not clearly show shorter products (Fig. 4a). Sequence analysis of the 22 shorter PCR products showed that 16 mutants resulted from simple deletions ranging from 109 to 3,964 bp. Zero to 6-bp microhomology was observed at the junctions in these mutants, indicating that a nonhomologous end-joining (NHEJ) model could explain the deletions

**Fig. 1 (Overleaf).** Creating assay systems to detect end-joining (EJ) and homologous recombination (HR) for repair of a double-strand break (DSB) at a I-*Sce*I site in the human thymidine kinase (*TK*) gene. **a:** Structure of the functional *TK* allele in TK6 cells, and construction of the targeting vectors. The functional allele of the TSCE5 cell line is modified with a 31-bp DNA insert, including the 18-bp I-*Sce*I site at a *Bgl*II site 75 bp upstream of exon 5. The TSCER2 cell line contains an additional point mutation (X) in exon 5 of the targeted allele, which results in an inactive the *TK* gene. **b:** PCR analysis of a DNA fragment with 164F and 196R primers. Because of the inserted DNA, the DNA from the TSCE5 cell line produces a 131-bp DNA fragment in addition to the original 100-bp fragment, and the larger product can be cleaved by I-*Sce*I endnuclease. **c:** Schematic representation of the experimental system. Closed and open rectangles represent the wild-type and mutant exons of the *TK* gene, respectively. When a DSB at the I-*Sce*I site is repaired by EJ, and it causes deletion in exon 5, TK-deficient mutants are isolated from TSCE5 cells in TFT medium. When HR repairs the DSB, TK-proficient revertants are generated from TSCER2 cells under HAT selection.

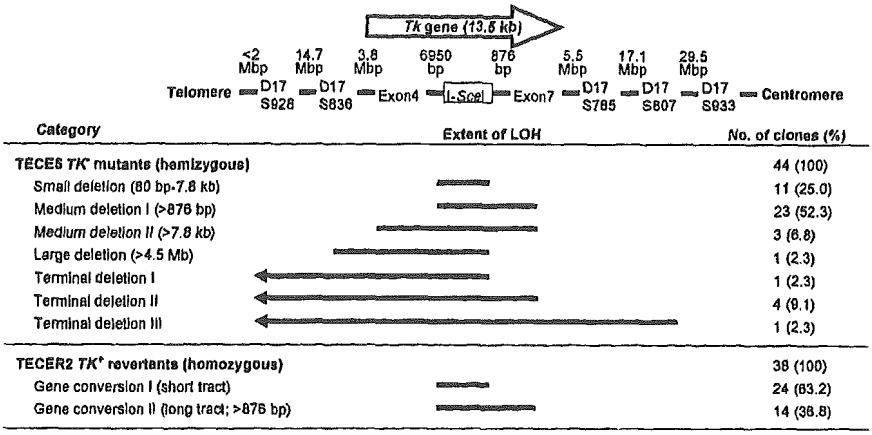


**Fig. 3.** Extent of (loss of heterozygosity (LOH) in thymidine kinase (TK)-deficient mutants from TSCE5 and TK-proficient revertants from TSCER2. Two frame-shift mutations in exons 4 and 7 of the *TK* gene and 5 microsatellite loci on chromosome 17q that are heteromorphic in the cell lines were used for the analysis. The human *TK* gene consists of 13.5 kb and maps to 17q23.2, oriented from telomere to centromere. The length of bars indicates the extent of LOH. Forty-four TSCE5 mutants and 36 TSCER2 revertants were analyzed.

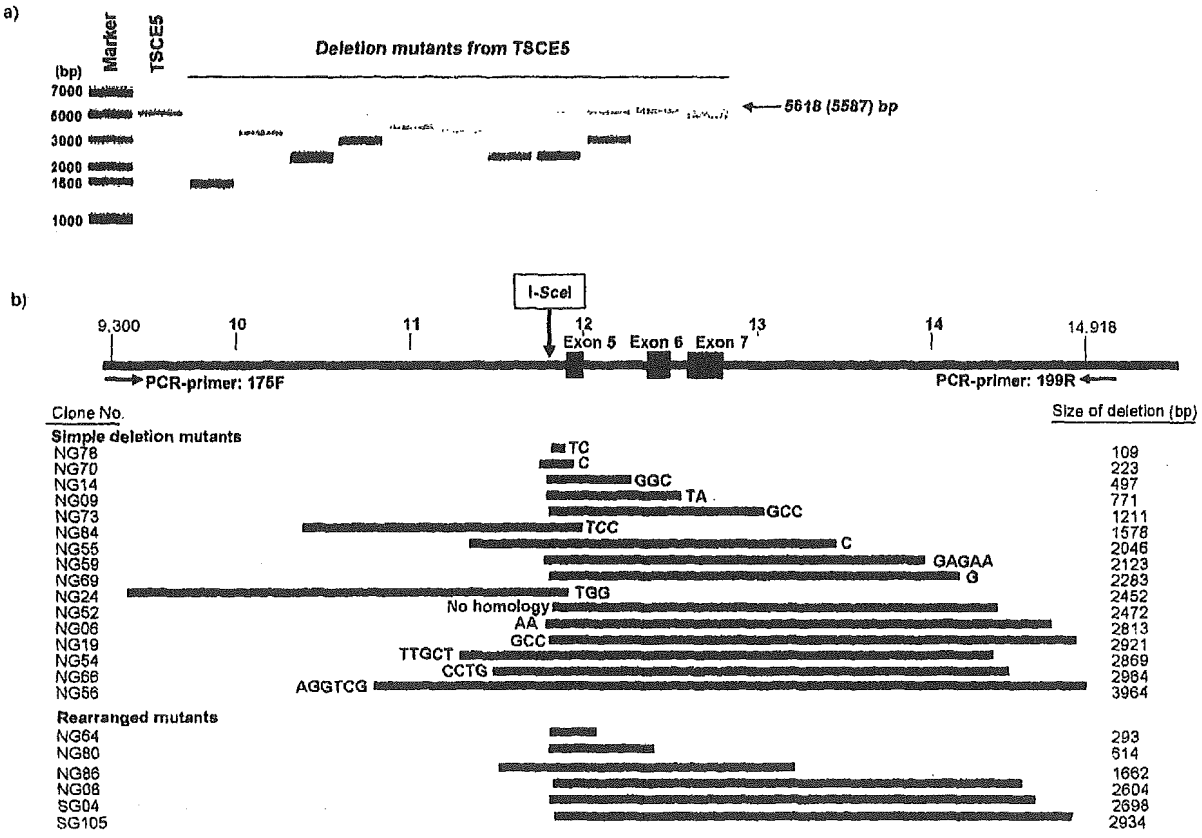


**Fig. 4.** Polymerase chain reaction (PCR) and sequence analysis of the regions flanking the *I-SceI* site in small deletion and medium deletion-I mutants (Fig. 3. ) from TSCE5 cells. **a:** PCR analysis of a DNA fragment involving exons 5, 6, and 7 of the thymidine kinase (*TK*) gene with primers 175F and 199R. The DNA from the TSCE5 cell line produces 5,587-bp and 5,618-bp DNA fragments. DNAs from TK-deficient TSCE5 mutants exhibit shorter DNA fragments caused by deletion. **b:** Twenty-two of 34 mutants contained shorter PCR products. The length of bars indicates the extent of deletion. Sixteen mutants exhibited simple deletions with microhomology sequences, which are indicated on the side of bars, and the other six mutants had deletions combined with complicated DNA rearrangements (Fig. 5).

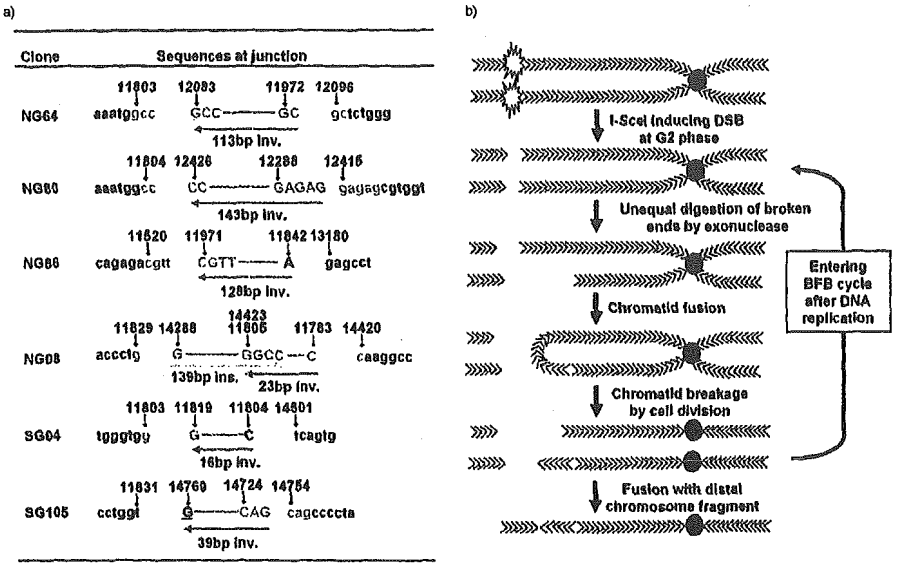


**Fig. 5.** Complicated DNA rearrangements in thymidine kinase (TK)-deficient mutants from TSCE5 cells. **a:** DNA sequences of the junctions of six mutants with complicated DNA rearrangements (Fig. 4). Sequences with small letters are outside of the junction. Blue-left arrows and green-right arrows show inverted and right directed sequences in parts of deleted region, respectively. Sequences indicated by red capitals indicate the microhomology at junctions. **b:** A model for mechanisms eliciting the complicated DNA rearrangements produced by double-strand breaks (DSBs). Two broken ends of DSBs on sister chromatids in $G_2$ phase cells are unequally processed by exonuclease, and fuse to each other to form a chromatid bridge. The dicentric chromatid is torn by cell division, producing daughter cells with broken chromosomes, which fuse with telomeric chromosome fragments. Some broken chromosomes enter a breakage-fusion-bridge (BFB) cycle, leading to more complicated rearrangements with inverted and right directed sequences at the junction.

[Haber, 2000; Jackson, 2002]. Interestingly, six other mutants exhibited complicated DNA rearrangements that involved a deletion combined with an inverted sequence that was part of the deleted sequence (Fig. 5a). Clone NG08 exhibited a particularly complicated rearrangement consisting of an inverted sequence and a forward sequence. Because these inverted sequences also joined through a 0- to 5-bp microhomology, EJ probably contributed to the rearrangement. We also examined these rearranged mutants by SKY analysis. There was, however, no apparent alteration in chromosome 17q and no translocated chromosome fragments derived from chromosome 17 in the mutants (data not shown).

### HR Always Resulted in Non-Crossing-Over Gene Conversion

We also analyzed 38 TSCER2 revertants. Every revertant showed LOH at the I-*Sce*I site accompanied by an increased band intensity of the intact allele (Fig. 1b). This means that HR between homologous chromosomes produced the revertants, as expected, resulting in homozygous LOH. Extended LOH analysis revealed that no revertant showed LOH at any polymorphic marker surrounding the *TK* gene (Fig. 3). Every LOH was limited to the *TK* gene, implying that these revertants were the result of gene conversion without crossing-over. The tract length of the gene conversion varied in the revertants. At least 14 (37%) of the revertants were generated by >876-bp tract gene conversion.

### No Small Deletions or Small Tract Gene Conversions Were Observed in Nonselected Cells

After transfecting TECS5 cells with the I-*Sce*I expression vector pCMV3xnls-I-*Sce*I, we isolated a total of 1,442 independent clones without TFT selection and analyzed their I-*Sce*I sites by PCR. All clones except one had the intact I-*Sce*I site and were identical to parental TSCE5 cells. The exceptional clone, however, had a deletion of >1 kb that included exons 5 and 6 (data not shown).

## DISCUSSION

### Contribution of EJ and HR for Repairing a Chromosome DSB

The assay system we established in the present study can trace the fate of a DSB in the human genome. We succeeded in integrating an I-*Sce*I site into an endogenous single-copy gene by two gene-targeting steps to minimize the introduction of other exogenous DNA sequences. It is likely that the DSB generated at the I-*Sce*I site was similar to DSBs

induced by low-dose irradiation in an intact genomic region, and the fate of the DSB seemed to depend on the physiological response to the exogenous DNA damage. The I-*Sce*I induced DSBs in $G_1$ phase were chromosomal breaks, while during late S and $G_2$ phases they were single or double chromatid breaks. EJ can operate throughout the cell cycle but may be more important during $G_1$ phase, while HR is a post-DNA-replication repair pathway [Johnson and Jasin, 2000; Hendrickson, 1997]. HR likely repairs chromatid breaks occurring in the late S and $G_2$ phases, and for chromosomal breaks that escape from EJ in the $G_1$ phase and turn into sister-chromatid breaks after DNA replication. Breaks on both sister chromatids can be repaired only by inter-allelic HR, although either chromatid break could be effectively repaired by sister-chromatid HR, which can not be demonstrated in our system [van Gent et al., 2001]. Because the human lymphoblastoid cells used in this study were unsynchronized and more than 50% were in $G_1$ phase [Little et al., 1995], the genetic consequences of DSB repair in the present system are mainly a reflection of chromosomal DSBs.

By transfecting the I-*Sce*I expression vector into the cells, TK-deficient mutants from TSCE5 cells and TK-proficient revertants from TSCER2 cells were recovered 130- and 200-fold more frequently than spontaneous mutants, respectively, suggesting that DSBs can stimulate inter-allelic HR as well as EJ. Because the revertant frequency was much less than the mutant frequency, however, almost all DSBs appear to be repaired by EJ. The relative contribution of EJ and HR for repairing DSBs in mammalian cells varies in the cells and the systems used to detect them, but EJ is the predominant mechanism for DSB repair in most cases [Takata et al., 1998; Essers et al., 2000]. Liang et al. [1998] and Johnson and Jasin [2000] demonstrated that approximately 30–50% of DSBs generated at an I-*Sce*I site in tandem repeated recombination substrates were repaired by HR, with the rest repaired by EJ. The system is, however, strongly biased in favor of detecting intra-chromosomal recombination between the repeated sequences. Almost 1% of DSBs in LINE-1 sequences (a repetitive element found throughout the mammalian genome at approximately $1 \times 10^5$ copies) was repaired by HR [Tremblay et al., 2000]. The contribution of HR for repairing chromosomal DSBs in a single copy mammalian gene must be quite low, however, because only the homologous allele is available as a recombination partner. Recently, Stark and Jasin [2003] estimated that an I-*Sce*I-induced DSB in a single-copy gene in mouse ES cells is repaired at least 1,000-fold more efficiently by EJ than by inter-allelic HR. Our present study strongly supported their estimation; nearly 100% of chromosomal DSBs were repaired by EJ in human TK6 cells, and HR rarely contributed to the repair.

The assay system described in the present study cannot recover every genetic consequence of EJ and HR. Because the I-*Sce*I site is inserted in intron 4 of the functional *TK* allele, in a position 75 bp upstream of exon 5, a small deletion caused by EJ that does not affect the TK function will not be recovered as a TFT-resistant mutant. Similarly, a small-tract gene conversion not extending to the point mutation in exon 5 (base 23 of exon 5) also will not be rescued in the reversion assay (Fig. 1a). If small deletions and small-tract gene conversions are the major products of EJ and HR, respectively, the mutants and revertants recovered in this assay system may not accurately reflect DSB repair. In fact, Lin et al. [1999] reported that I-*Sce*I induced DSBs in mouse chromosomes were mainly repaired by EJ, resulting in very few nucleotide deletions. To clarify this issue, we isolated 1,442 independent clones from TSCE5 cells without drug selection after transfection with the I-*Sce*I expression vector and examined their I-*Sce*I site. No small deletions or small-tract gene conversions were observed; the one mutant clone detected had a 1-kb deletion, which should have been detected as a TK-deficient mutant. Although the efficiency of inducing DSBs by transfection of the I-*Sce*I expressing vector is not clear and the number of analyzed clones may not be sufficient, this result would indicate that our assay system detected most of the genetic consequences resulting from the repair of DSBs and was not strongly biased in favor of specific genetic events.

## Genetic Consequences of Chromosomal DSBs Repaired by EJ

Around 70% (16/22) of the small deletions we analyzed by PCR and sequencing exhibited simple deletions ranging from 109 to 3,964 bp with a 0- to 6-bp microhomology at the junction of the deletion. These deletions can be explained by an NHEJ model, which is a general EJ mechanism found in mammalian cells as well as in other species [Haber, 2000; Jackson, 2002]. Single-strand annealing (SSA), which is a special form of HR that works efficiently on repeated sequences flanking DSBs in yeast and mammalian cells [Paques and Haber, 1999; Lin et al., 1990], can cause simple deletions in a nonconservative manner. This mechanism can be excluded for generating the deletions, however, because it would need at least a 30-bp homology at the sequence junctions [Sugawara et al., 2000]. SSA may not function for DSB repair in a single-copy gene, but it may have been responsible for some of the unanalyzed large deletions. In contrast, six other mutants exhibited complicated DNA rearrangements in which a deletion was combined with an inverted sequence that was part of the deleted sequence (Fig. 5a). Because these inverted sequences also joined through 1- to 5-bp microhomologies, EJ probably contributed to the rearrangements. We speculate that some DSBs occurring in late S or $G_2$ phase could lead to the rearrangements (Fig. 5b). DSBs induced by I-*Sce*I expression occur at the same position on both sister chromatids after DNA replication. The ends of the broken sister chromatids that are unequally processed by exonuclease may

occasionally fuse to each other to form a chromatid bridge. A dicentric chromatid torn by cell division produces daughter cells with broken chromosomes, and the telomeric chromosome fragment may fuse again. Clone NG08 exhibited a more complicated rearrangement consisting of an inverted sequence and a forward sequence, implying that a breakage-fusion-bridge (BFB) cycle occurred. A BFB cycle resulting from telomere loss is associated with chromosome instability and sometimes results in high-copy gene amplification or nonreciprocal translocation, which is commonly observed in tumor cells [Kuo et al., 1994; Coquelle et al., 1997]. These specific DNA rearrangements, however, may be observed in I-*Sce*I-induced mutagenesis at a high frequency because of the simultaneous occurrence of DSBs at the same position on both sister chromatids. In spite of the complex DNA rearrangement, these mutants did not reveal any gross changes in chromosome 17q. Lo et al. [2002] and Pipiras et al. [1998] reported that DSBs induced by I-*Sce*I cause chromosomal instability, and sometimes result in large interstitial deletions and intra-chromosomal amplifications through a BFB cycle. Other unanalyzed mutants from TSCE5 in this study, which are expected to have deletions of ≥5 kb, may show gross structural changes initiated by a BFB cycle, although they would be a minor consequence of DSBs.

### Genetic Consequences of Chromosomal DSBs Repaired by HR

In the HR repair model, recombinational intermediates (Holliday junctions) may be resolved as a reciprocal exchange (crossing-over) or a nonreciprocal transfer of genetic information (gene conversion without crossing-over) [Szostak et al., 1983]. Both products appear equally for meiotic recombination at some loci [Cromie et al., 2001]. Molecular analysis of 38 revertants from TSCER2 cells, however, clearly demonstrated that gene conversion was preferred for repairing DSBs, because no revertants showed LOH at any of the distal microsatellite markers. HR for repairing DSBs generally occurs during postreplication, and inter-allelic recombination is also thought to occur between chromatids in the late S and $G_2$ phase. Theoretically, reciprocal exchange can produce revertants that retain distal heterozygosity if the two chomatids involved as recombination partners are co-segregated by cell division. Because co-segregation presumably will occur 50% of the time, resulting in LOH at distal markers, the participation of reciprocal exchange for the generation of these revertants can be excluded. In contrast, most HR products occurring spontaneously or induced by ionizing irradiation in autosomal recessive gene mutation assays in mouse and human cells are the result of reciprocal exchange [Honma et al., 1997b, 2000, 2001]. This may be because of the strong bias for recovery of HR products with crossing-over involving nontargeted mutagenesis; reciprocal exchange that affects a particular target (e.g., the *TK* gene) must occur at relatively a low frequency. Quintana et al. [2001] developed a cell line from TK6 that has a compound heterozygous *TK* gene (*TK* $^{+/-}$) and examined TK-proficient revertants induced by ionizing irradiation and a chemical mutagen. These investigators also did not recover any revertants with crossing-over, and they estimated that non-crossing-over is approximately 700-fold more frequent than reciprocal exchanges on a yield-per-kilobase basis. A preference for recovery of gene conversion rather than reciprocal exchanges in mitosis also was reported in yeast and mammalian cells [Paques and Haber, 1999; Cromie et al., 2001]. In yeast, however, about 10% of inter-allelic HR events involved crossing-over [Nickoloff et al., 1999], while almost all inter-allelic HR in mammalian cells was of a non-crossing-over type [Stark and Jasin, 2003]. Thus, Holliday intermediates must be resolved with bias, especially in mammalian cells. The strong suppression of reciprocal exchanges may contribute to the maintenance of genomic integrity because reciprocal exchange could bring about large-scale genetic alterations, including translocations [Richardson et al., 1998].

Although the present study showed that the contribution of HR for repairing chromosomal DSBs is quite low, HR must be essential for maintaining genomic integrity in mammalian cells. Knocking out *Rad51* and other genes involved in HR, such as *Rad52*, *Xrcc2*, and *Xrcc3*, is lethal, enhances sensitivity to ionizing irradiation and chemicals, and/or influences the fidelity of HR [Rijkers et al., 1998; Cui et al., 1999; Takata et al., 2001; Sale et al., 2001; Brenneman et al., 2002]. These observations indicate that HR has an important role in overcoming some genetic stresses. Most spontaneous DSBs in mammalian cells is thought to be produced by replication stress rather than exogenous effects [Haber, 1999]. Single-strand breaks are frequently converted during nucleotide and base excision repair to DSBs when replication folks are encountered. These types of DSBs could be repaired efficiently by HR between sister chromatids in the late S and $G_2$ phases, which would be critical for maintaining genomic integrity as well as cell viability. Thus, HR may be important for repairing chromatid breaks generated by the replication stress [Kadyk and Hartwell, 1992], but not for chromosome breaks. The role of inter-allelic HR remains unclear, although it is clearly induced by DSBs. Inter-allelic HR contributes greatly to genomic instability, in particular LOH in tumorigenesis, and may be associated with genetic and environmental factors [Lasko et al., 1991; Moynahan and Jasin, 1997].

We conclude that almost all chromosomal DSBs are repaired by EJ in human cells, and that when HR is involved, it is in the form of gene conversion without crossing-over. These findings strongly support the preferences of mammalian DSB repair pathways reported previously. The present system established in the present study can trace the fate of DSBs in mammalian cells quantitatively as well as qualitatively, and holds promise for elucidating genetic and

environmental factors that influence DSB repair [Palmer et al., 2003].

## ACKNOWLEDGMENTS

The authors thank Dr. Jac A. Nickoloff (University of New Mexico School of Medicine, New Mexico) for providing the I-*Sce*I expression vector, pCMV3xnls-I-*Sce*I. We also thank Dr. Robert H. Heflich (National Center for Toxicological Research, Arkansas) for helpful comments and review of the manuscript.

## REFERENCES

Brenneman MA, Wagener BM, Miller CA, Allen C, Nickoloff JA. 2002. XRCC3 controls the fidelity of homologous recombination: roles for XRCC3 in late stages of recombination. Mol Cell 10:387–395.

Coquelle A, Pipiras E, Toledo F, Buttin G, Debatisse M. 1997. Expression of fragile sites triggers intrachromosomal mammalian gene amplification and sets boundaries to early amplicons. Cell 89:215–225.

Cromie GA, Connelly JC, Leach DR. 2001. Recombination at double-strand breaks and DNA ends: conserved mechanisms from phage to humans. Mol Cell 8:1163–1174.

Cui X, Brenneman M, Meyne J, Oshimura M, Goodwin EH, Chen DJ. 1999. The XRCC2 and XRCC3 repair genes are required for chromosome stability in mammalian cells. Mutat Res 434:75–88.

Elliott B, Richardson C, Winderbaum J, Nickoloff JA, Jasin M. 1998. Gene conversion tracts from double-strand break repair in mammalian cells. Mol Cell Biol 18:93–101.

Essers J, van Steeg H, de Wit J, Swagemakers SM, Vermeij M, Hoeijmakers JH, Kanaar R. 2000. Homologous and non-homologous recombination differentially affect DNA damage repair in mice. EMBO J 19:1703–1710.

Giver CR, Grosovsky AJ. 1997. Single and coincident intragenic mutations attributable to gene conversion in a human cell line. Genetics 146:1429–1439.

Grosovsky AJ, Walter BN, Giver CR. 1993. DNA-sequence specificity of mutations at the human thymidine kinase locus. Mutat Res 289: 231–243.

Haber JE. 1995. In vivo biochemistry: physical monitoring of recombination induced by site-specific endonucleases. BioEssays 17:609–620.

Haber JE. 1999. DNA recombination: the replication connection. Trends Biochem Sci 24:271–275.

Haber JE. 2000. Partners and pathways repairing a double-strand break. Trends Genet 16:259–264.

Hendrickson EA. 1997. Cell-cycle regulation of mammalian DNA double-strand-break repair. Am J Hum Genet 61:795–800.

Honma M, Hayashi M, Sofuni T. 1997a. Cytotoxic and mutagenic responses to X-rays and chemical mutagens in normal and p53-mutated human lymphoblastoid cells. Mutat Res 374:89–98.

Honma M, Zhang LS, Hayashi M, Takeshita K, Nakagawa Y, Tanaka N, Sofuni T. 1997b. Illegitimate recombination leading to allelic loss and unbalanced translocation in p53-mutated human lymphoblastoid cells. Mol Cell Biol 17:4774–4781.

Honma M, Momose M, Tanabe H, Sakamoto H, Yu Y, Little JB, Sofuni T, Hayashi M. 2000. Requirement of wild-type p53 protein for maintenance of chromosomal integrity. Mol Carcinog 28:203–214.

Honma M, Momose M, Sakamoto H, Sofuni T, Hayashi M. 2001. Spindle poisons induce allelic loss in mouse lymphoma cells through mitotic non-disjunction. Mutat Res 493:101–114.

Honma M, Tadokoro S, Sakamoto H, Tanabe H, Sugimoto M, Furuichi Y, Satoh T, Sofuni T, Goto M, Hayashi M. 2002. Chromosomal instability in B-lymphoblastoid cell lines from Werner and Bloom syndrome patients. Mutat Res 520:15.

Jackson SP. 2002. Sensing and repairing DNA double-strand breaks. Carcinogenesis 23:687–696.

Jackson SP, Jeggo PA. 1995. DNA double-strand break repair and V(D)J recombination: involvement of DNA-PK. Trends Biochem Sci 20: 412–415.

Johnson RD, Jasin M. 2000. Sister chromatid gene conversion is a prominent double-strand break repair pathway in mammalian cells. EMBO J 19:3398–3407.

Johnson RD, Jasin M. 2001. Double-strand-break-induced homologous recombination in mammalian cells. Biochem Soc Trans 29:196–201.

Kadyk LC, Hartwell LH. 1992. Sister chromatids are preferred over homologs as substrates for recombinational repair in *Saccharomyces cerevisiae*. Genetics 132:387–402.

Khanna KK, Jackson SP. 2001. DNA double-strand breaks: signaling, repair and the cancer connection. Nat Genet 27:247–254.

Kuo MT, Vyas RC, Jiang LX, Hittelman WN. 1994. Chromosome breakage at a major fragile site associated with P- glycoprotein gene amplification in multidrug-resistant CHO cells. Mol Cell Biol 14: 5202–5211.

Lasko D, Cavenee W, Nordenskjold M. 1991. Loss of constitutional heterozygosity in human cancer. Annu Rev Genet 25:281–314.

Liang F, Han M, Romanienko PJ, Jasin M. 1998. Homology-directed repair is a major double-strand break repair pathway in mammalian cells. Proc Natl Acad Sci USA 95:5172–5177.

Liber HL, Thilly WG. 1982. Mutation assay at the thymidine kinase locus in diploid human lymphoblasts. Mutat Res 94:467–485.

Lin FL, Sperle K, Sternberg N. 1990. Intermolecular recombination between DNAs introduced into mouse L cells is mediated by a nonconservative pathway that leads to crossover products. Mol Cell Biol 10:103–112.

Lin Y, Lukacsovich T, Waldman AS. 1999. Multiple pathways for repair of DNA double-strand breaks in mammalian chromosomes. Mol Cell Biol 19:8353–8360.

Little JB, Nagasawa H, Keng PC, Yu Y, Li CY. 1995. Absence of radiation-induced G1 arrest in two closely related human lymphoblast cell lines that differ in p53 status. J Biol Chem 270:11033–11036.

Lo AW, Sprung CN, Fouladi B, Pedram M, Sabatier L, Ricoul M, Reynolds GE, Murnane JP. 2002. Chromosome instability as a result of double-strand breaks near telomeres in mouse embryonic stem cells. Mol Cell Biol 22:4836–4850.

Moynahan ME, Jasin M. 1997. Loss of heterozygosity induced by a chromosomal double-strand break. Proc Natl Acad Sci USA 94: 8988–8993.

Nickoloff JA, Sweetser DB, Clikeman JA, Khalsa GJ, Wheeler SL. 1999. Multiple heterologies increase mitotic double-strand break-induced allelic gene conversion tract lengths in yeast. Genetics 153:665–679.

Palmer S, Schildkraut E, Lazarin R, Nguyen J, Nickoloff JA. 2003. Gene conversion tracts in *Saccharomyces cerevisiae* can be extremely short and highly directional. Nucleic Acids Res 31:1164–1173.

Paques F, Haber JE. 1999. Multiple pathways of recombination induced by double-strand breaks in *Saccharomyces cerevisiae*. Microbiol Mol Biol Rev 63:349–404.

Pipiras E, Coquelle A, Bieth A, Debatisse M. 1998. Interstitial deletions and intrachromosomal amplification initiated from a double-strand break targeted to a mammalian chromosome. EMBO J 17:325–333.

Quintana PJ, Neuwirth EA, Grosovsky AJ. 2001. Interchromosomal gene conversion at an endogenous human cell locus. Genetics 158:757–767.

Richardson C, Moynahan ME, Jasin M. 1998. Double-strand break repair

by interchromosomal recombination: suppression of chromosomal translocations. Genes Dev 12:3831–3842.

Rijkers T, Van Den OJ, Morolli B, Rolink AG, Baarends WM, Van Sloun PP, Lohman PH, Pastink A. 1998. Targeted inactivation of mouse RAD52 reduces homologous recombination but not resistance to ionizing radiation. Mol Cell Biol 18:6423–6429.

Sale JE, Calandrini DM, Takata M, Takeda S, Neuberger MS. 2001. Ablation of XRCC2/3 transforms immunoglobulin V gene conversion into somatic hypermutation. Nature 412:921–926.

Sargent RG, Brenneman MA, Wilson JH. 1997. Repair of site-specific double-strand breaks in a mammalian chromosome by homologous and illegitimate recombination. Mol Cell Biol 17:267–277.

Stark JM, Jasin M. 2003. Extensive loss of heterozygosity is suppressed during homologous repair of chromosomal breaks. Mol Cell Biol 23:733–743.

Sugawara N, Ira G, Haber JE. 2000. DNA length dependence of the single-strand annealing pathway and the role of *Saccharomyces cerevisiae* RAD59 in double-strand break repair. Mol Cell Biol 20:5300–5309.

Szostak JW, Orr-Weaver TL, Rothstein RJ, Stahl FW. 1983. The double-strand-break repair model for recombination. Cell 33:25–35.

Taghian DG, Nickoloff JA. 1997. Chromosomal double-strand breaks induce gene conversion at high frequency in mammalian cells. Mol Cell Biol 17:6386–6393.

Takata M, Sasaki MS, Sonoda E, Morrison C, Hashimoto M, Utsumi H, Yamaguchi-Iwai Y, Shinohara A, Takeda S. 1998. Homologous recombination and non-homologous end-joining pathways of DNA double-strand break repair have overlapping roles in the maintenance of chromosomal integrity in vertebrate cells. EMBO J 17: 5497–5508.

Takata M, Sasaki MS, Tachiiri S, Fukushima T, Sonoda E, Schild D, Thompson LH, Takeda S. 2001. Chromosome instability and defective recombinational repair in knockout mutants of the five Rad51 paralogs. Mol Cell Biol 21:2858–2866.

Tremblay A, Jasin M, Chartrand P. 2000. A double-strand break in a chromosomal LINE element can be repaired by gene conversion with various endogenous LINE elements in mouse cells. Mol Cell Biol 20:54–60.

Van Dyck E, Stasiak AZ, Stasiak A, West SC. 1999. Binding of double-strand breaks in DNA by human Rad52 protein. Nature 398:728–731.

van Gent DC, Hoeijmakers JH, Kanaar R. 2001. Chromosomal stability and the DNA double-stranded break connection. Nat Rev Genet 2:196–206.

Cytogenet Genome Res 104:299–303 (2004)
DOI: 10.1159/000077506

Cytogenetic and Genome Research

# A liver micronucleus assay using young rats exposed to diethylnitrosamine: methodological establishment and evaluation

H. Suzuki,[a] T. Shirotori,[b] and M. Hayashi[c]

[a] Ina Research Inc., Nagano; [b] The Collaborative Study Group of the Micronucleus Test – Mammalian Mutagenicity Study Group/Japanese Environmental Mutagen Society; [c] Division of Genetics and Mutagenesis, National Institute of Health Sciences, Tokyo (Japan)

**Abstract.** We have developed a simple liver micronucleus assay using young rats (up to 4 weeks old) to assess cytogenetic damage of chemicals in liver cells. Diethylnitrosamine (DEN) was used as a model rodent hepatocarcinogen in this study. Compared to the partial hepatectomy method most commonly used for the liver micronucleus assay, the present assay method showed equal or even higher practicability. The young rat liver micronucleus assay was also characterized for rat strain differences, sampling time after treatment, single treatment vs. split treatment, age of animals, administration route, and staining method. Although based on one model chemical, we propose an acceptable protocol for the micronucleus assay using young rat liver as follows: Up to 4-week-old rats should be used; oral or intraperitoneal administration can be used; single or repeated treatment protocols can be applied; sampling time is 3–5 days after the last treatment; hepatocytes are prepared by the collagenase perfusion method; and cells are stained with the AO-DAPI double staining method.



Micronucleus assays have been widely performed using bone marrow cells to assess the clastogenic potential of chemicals in vivo. Since bone marrow (BM) is one of the continuously proliferating tissues in adult animals, it has been used as a common target organ for cytogenetic studies. However, it is well known that some compounds need metabolic activation in the liver, and it has been pointed out that some pro-mutagens elicit a negative response in the BM micronucleus assay (Morita et al., 1997). It may be considered that some active metabolites have a very short lifespan and do not reach the BM at sufficient concentrations to induce micronuclei. In fact, some rodent liver carcinogens, including di-alkyl-nitrosamines, nitro aromatic compounds, and azo derivatives, gave negative results in a BM assay (Angelosanto, 1995). It is worthwhile, therefore, to consider the selection of other organs for evaluating genotoxicity of test chemicals, especially the liver for detecting liver carcinogens. The use of suitable organs for genotoxicity determination is also recommended in the guidance proposed by the Committee on Mutagenicity of Chemicals in Food, Consumer Products and the Environment (Committee on the Mutagenicity of Chemicals, 2000).

In recent years, various investigators have tried to develop a liver micronucleus assay. Due to extremely low mitotic activity in adult animals, procedures require mitotic stimulation of liver cells together with treatment of animals with test chemicals. Tates et al. (1980) reported a method comprising partial hepatectomy (PH) before or after chemical treatment for the liver micronucleus assay. The division of hepatocytes is stimulated by PH, and positive responses were obtained in induction of micronuclei in liver cells after treatment with liver carcinogens that gave negative results in the BM assay. Other investigators also evaluated the chemical clastogenicity potential in the liver by the PH method (Cliet et al., 1989; Roy and Das, 1990; Mere-

Received 22 August 2003; manuscript accepted 15 December 2003.

Request reprints from Dr. Hiroshi Suzuki, Ina Research Inc.
2148-188 Nishiminowa, Ina-shi, Nagano 399-4501 (Japan)
telephone: +81-265-73-8611; fax: +81-265-73-8612
e-mail: h-suzuki@ina-research.co.jp





0301–0171/04/1044–0299$21.00/0

Accessible online at:
www.karger.com/cgr

to et al., 1994; Zhurkov et al., 1996). There are, however, two shortcomings in the PH method: 1) Technically it is not easy to perform successful hepatectomy on all animals used in the assay, and 2) it has been reported that cytochrome P450, styrene mono-oxygenase, epoxide hydrolase, and glutathione-S-epoxide transferase activities decreased by 50, 35, 50, and 35%, respectively 12 h after PH (Rossi et al., 1987).

Another method used 4-acetyl aminofluorene (4AAF), a mitogen for liver cells (Braithwaite and Ashby, 1988), to activate cell proliferation. In this method, the possibility of interaction with the test chemical has not been ignored (Parton and Garriott, 1997). An in vivo/in vitro assay system has also been reported, i.e., after treatment of animals with test chemicals in vivo, hepatocytes were collected and primary cell cultures were established with growth factors before cell harvest for slide preparation (Sawada et al., 1991). However, this in vivo/in vitro method is labor-intensive, costly and time consuming; thus it has not been used as a routine method to evaluate chemical clastogenicity in the liver.

The use of proliferating tissue is a prerequisite for the micronucleus assay. In 4-week-old rats, the hepatocytes are still proliferating, and the percentage of S phase cells is more than 40 times higher than in adult rat liver (Parton and Garriott, 1997). Sipes and Gandolfi (1993) reported that P450 levels reach a maximum at 4 weeks of age in the rat. Considering these points, we developed and evaluated the young (4-week-old) rat liver micronucleus assay. We used diethylnitrosamine (DEN), which is a well-known rodent liver carcinogen, as a model compound. DEN was negative in the conventional BM micronucleus assay (Morita et al., 1997), but positive in the liver micronucleus assay using the PH method (Tates et al., 1980). This paper describes the comparison of the PH and young rat methods and investigations of technical points in the young rat liver micronucleus assay.

## Materials and methods

*Animals*

Male Fischer 344 (F344) and Sprague Dawley (SD) rats were purchased from Charles River Japan. The animals were housed under a 12-hour light-dark cycle and allowed free access to food and water.

*Chemicals*

Diethylnitrosamine (DEN, CAS No. 55-18-5), was purchased from Wako Pure Chemical Industries, Ltd. (Osaka, Japan). DEN was dissolved in physiological saline immediately before treatment and given once or twice by intraperitoneal injection or gavage to rats.

*Comparison of the young rat method with the partial hepatectomy (PH) method*

F344 or SD rats were treated orally with 50 mg/kg of DEN at 3 or 4 weeks of age in the young rat method, and at 6 weeks of age in the PH method. In the former method, slide preparations were made 2–5 days after single treatment, and peripheral blood samples were collected and supravitally stained with acridine orange (AO)-coated slides (Hayashi et al., 1990) before and 1, 2, and 3 days after treatment. In the latter method, PH was performed 7 days after treatment, and the slides were prepared 2–5 days after PH.

*Dose dependency and age effect*

DEN at dose levels of 12.5, 25, and 50 mg/kg was administered to 4-week-old rats, and hepatocytes were isolated 5 days after treatment. To investigate the effect of age, F344 rats at 3–9 weeks of age were treated with DEN (50 mg/kg) once and slide preparations were made on the 5th day after treatment as with the dose-response assay.

*Administration route difference and treatment times*

4-week-old F344 rats were treated by gavage or intraperitoneally with DEN once at 40 mg/kg or twice at 20 mg/kg with a 24-hour interval. Hepatocytes were isolated 2–5 days after the last treatment.

*Preparation of hepatocytes*

Hepatocytes were isolated from anesthetized rats by the collagenase perfusion method, rinsed with 10% neutral buffered formalin 2 or 3 times and centrifuged at 50 *g* (500 rpm) for 1 min (Cliet et al., 1989). Hepatocytes were suspended with 10% neutral buffered formalin and stored in a refrigerator until analysis. In the case of PH, two-thirds of the liver was removed according to the published method (Higgins and Anderson, 1931). The hepatocytes were suspended with 10% neutral buffered formalin, and kept in a refrigerator until analysis.

*Microscopy and micronucleus determination*

Immediately prior to analysis, 10–20 µl of hepatocyte suspensions were mixed with an equal volume of AO-4′,6-diamidino-2-phenylindole dihydrochloride (DAPI) stain solution for fluorescent microscopy. The AO-DAPI stain solution contains one part of 500 µg/ml of AO aqueous solution and one part of 10 µg/ml of DAPI aqueous solution. Approximately 10–20 µl of stained hepatocyte suspension was dropped onto a glass slide and covered with a coverslip (24 × 40 mm).

Hepatocytes were analyzed under a fluorescent microscope (×400 or higher) equipped with a UV excitation system. The number of micronucleated hepatocytes (MNHEPs) was recorded based on analysis of 2000 hepatocytes (in two fields) from each animal. In accordance with the methods of Braithwaite and Ashby (1988) and Cliet et al. (1989), the following classification criteria for MNHEPs were used: Round or distinct micronuclei stained with the same color as the nuclei, with diameters of 1/4 or less that of the main nuclei. The number of mitotic cells was also counted in 1000 hepatocytes in each animal to determine the mitotic index (MI) for administration route or treatment time differences. Mitotic cells were defined as cells at any stage from prophase to telophase.

*Peripheral blood micronucleus assay*

5–10 µl of peripheral blood samples were collected from the tail vein and dropped on AO-coated slides (Hayashi et al., 1990), covered with a coverslip and stored overnight in a refrigerator until analysis. Reticulocytes supravitally stained with AO were analyzed under a fluorescent microscope (×600 or higher) equipped with a blue light excitation system. The number of micronucleated reticulocytes (MNRETs) was recorded by evaluation of 2000 reticulocytes in two fields per animal.

*Statistical analysis*

The incidences of micronucleated hepatocytes or reticulocytes were analyzed statistically by using Kastenbaum's and Bowman's tables (Kastenbaum and Bowman, 1970).

## Results

*AO-DAPI double fluorescent staining*

Figure 1 shows fluorescent microphotographs of nuclei in young rat hepatocytes stained with AO alone (Fig. 1a), DAPI alone (Fig. 1c), and combination of AO and DAPI (Fig. 1b). Compared to AO or DAPI alone, the double staining allows better distinction of micronuclei and cytoplasm.

*Comparison of the young rat method with the partial hepatectomy method*

The results of the assay with DEN at 50 mg/kg are shown in Fig. 2. Both methods revealed significant increases in the numbers of MNHEPs in comparison with concurrent controls. The frequencies of MNHEPs in young rats were generally higher

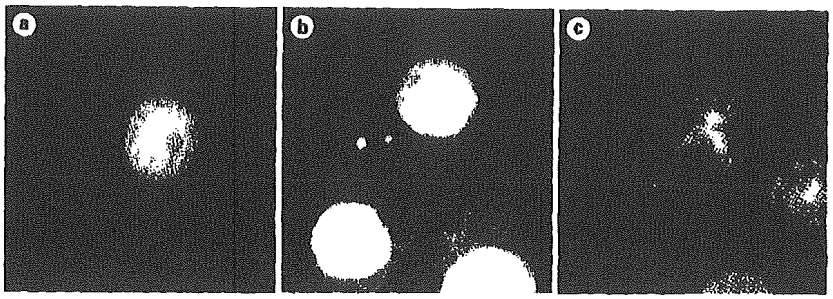


**Fig. 1.** Fluorescent microphotographs of hepatocyte nuclei from young rats stained with (**a**) AO alone, (**b**) a combination of AO and DAPI, and (**c**) DAPI alone.

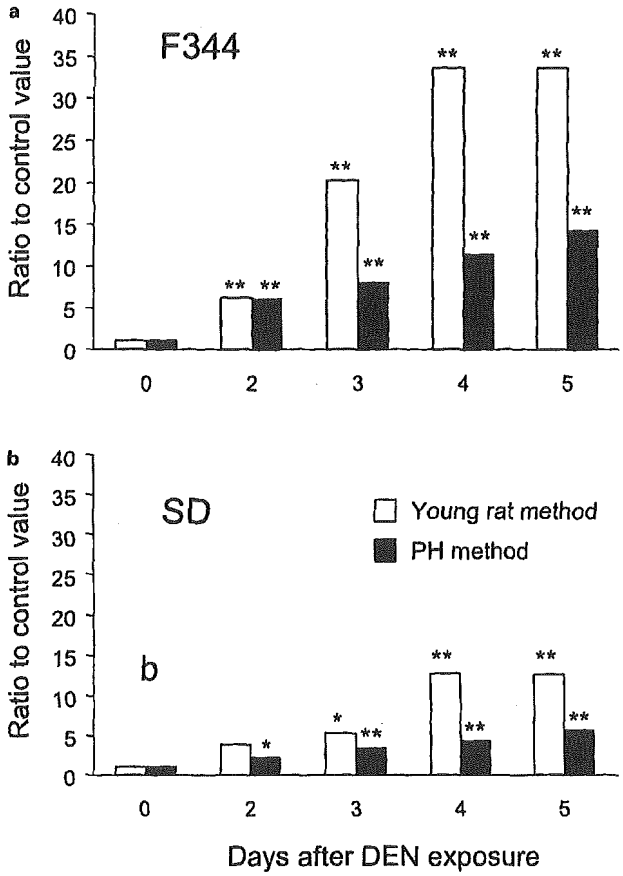


**Fig. 2.** Frequencies of MNHEPs (micronuclei/1000 hepatocytes) 2 to 5 days after administration of 50 mg/kg DEN to (**a**) F344 rats and (**b**) SD rats in the young rat method and PH method. Mean of 4–5 animals. * $P < 0.05$, ** $P < 0.01$, significantly different from the concurrent solvent control.

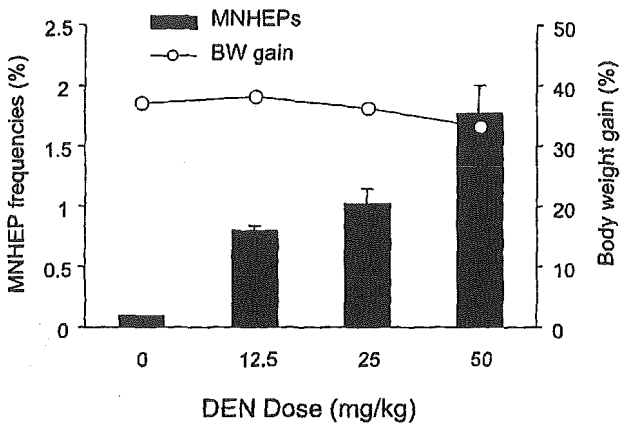


**Fig. 3.** MNHEP frequencies (evaluation of 2000 hepatocytes) 5 days after administration of DEN (12.5, 25 and 50 mg/kg) to F344 rats (column with standard deviation bar). Body weight (BW) gain was only marginally affected at the highest dose.

than those of the PH method and it was shown that the MNHEP frequencies of F344 rats (Fig. 2a) were higher than those of SD rats (Fig. 2b) in both methods. There was no statistically significant difference in MNRET induction observed in peripheral blood at any treatment time in either F344 or SD rats (data not shown).

*Dose dependency and age effect*

The MNHEP frequencies after administration of DEN (12.5, 25, 50 mg/kg) to 4-week-old F344 male rats increased dose dependently and reached approximately 9- to 20-fold the concurrent solvent control (Fig. 3). During this study, the rate of body weight gain was only marginally decreased at the highest DEN dose. The MNHEP frequency after 50 mg/kg DEN administration to F344 rats aged between 3 and 9 weeks decreased age-dependently, with the highest value (2.3%) at 3 weeks of age, and lowest (0.17%) at 9 weeks of age (Fig. 4).

*Route difference and treatment times*

To determine the influence of administration route, DEN was given either orally or intraperitoneally to 4-week-old F344 rats. MNHEP frequency was similar for both routes, 2–5 days after single (40 mg/kg) or the second treatment for a split-dose (2 × 20 mg/kg) regime (Fig. 5a, b). The MNHEP frequency increased depending on the time after DEN treatment (up to 5 days). On days 2, 3, and 4, split DEN dosing resulted in higher MNHEP frequencies compared to the single dose protocol. Mitotic cells were observed in 1.2 ± 0.30% to 1.5 ± 0.74% of cells in the solvent control group 5 days after treatment, and in

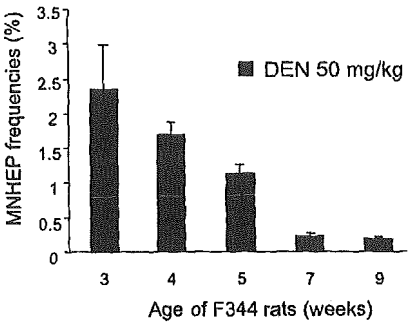


**Fig. 4.** MNHEP frequencies (evaluation of 2000 hepatocytes) after administration of 50 mg/kg DEN to F344 rats aged 3 to 9 weeks. Data are the mean of five animals with standard deviation.

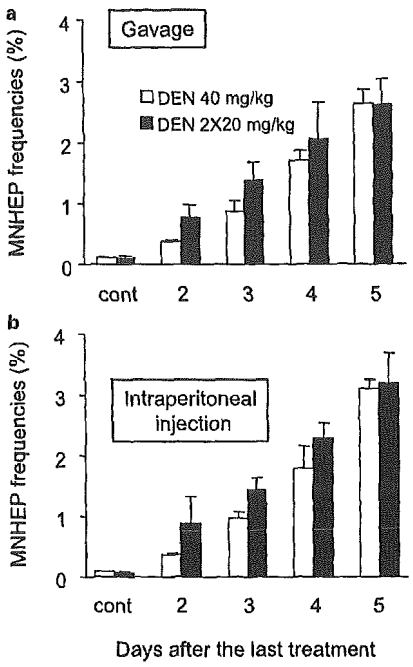


**Fig. 5.** DEN-induced MNHEP frequency (evaluation of 2000 hepatocytes) 2 to 5 days after a single 40 mg/kg dose or two 20 mg/kg doses 24 h apart in 4-week-old F344 rats by **(a)** gavage or **(b)** intraperitoneal injection. Results are the mean of five animals with standard deviation.

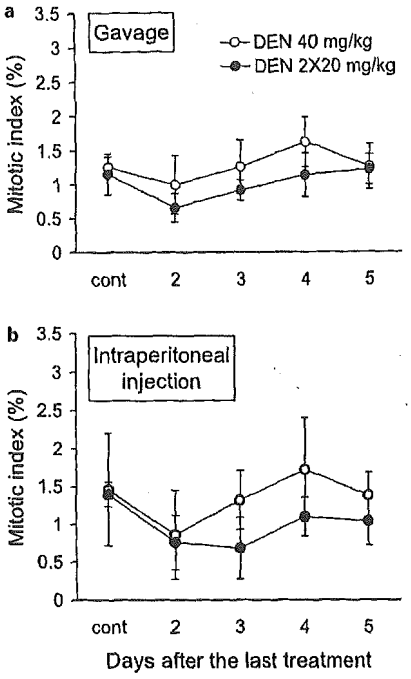


**Fig. 6.** Frequencies of mitotic indexes (evaluation of 1000 hepatocytes) 2 to 5 days after a single 40 mg/kg dose or two 20 mg/kg doses 24 h apart in 4-week-old F344 rats by **(a)** gavage or **(b)** intraperitoneal injection. Results are the mean of five animals with standard deviation.

0.7 ± 0.21% to 1.7 ± 0.68% of cells in the DEN group (Fig. 6a, b). The incidence of metaphase cells tended to be lower after the double treatment of DEN.

## Discussion

Since Tates et al. reported a liver micronucleus assay in 1980, a number of variations have been published (Cliet et al., 1989; Roy and Das, 1990; Mereto et al., 1994; Zhurkov et al., 1996). In these studies, the PH method, the chemical mitogens method, and an in vivo/in vitro method have been applied to assess micronucleus induction in liver cells. These methods have been used on a case by case basis, but they have not been used routinely for evaluation of genotoxicity of chemicals. Some criticisms of these methods are 1) introduction of abnormal physiological conditions (e.g., PH method), 2) increased unknown factors as a result of interaction between test chemical and mitogen, 3) laborious and time-consuming (e.g., *in vivo/in vitro* method). We have thus paid attention to the method based on proliferating activity of liver cells in young rats up to about 4 weeks of age. Although the method using young rat liver was reported by Parton and Garriott (1997), it has not been well characterized and evaluated.

We consider the young rat liver micronucleus assay method as advantageous because it does not require any physical injury such as PH, nor pretreatment with mitogens that may interact with a test substance, nor setting up of primary culture that also may cause damage to the target cells. Therefore, we propose to use the present method as a tool for evaluation of chemical genotoxicity that may occur in the liver.

As shown in Fig. 6, we confirmed that there were many mitotic cells in the liver of 4-week-old rats. The mitotic index (MI) observed in the present study was comparable to that reported by Parton and Garriott (1997). As shown in Fig. 4, the incidence of MNHEP decreased with the age of the rats. This can be explained by an age-related decrease in proliferation of hepatocytes and dilution of the cells with micronuclei with undivided normal hepatocytes. This phenomenon was also observed in the PH method. The MI in regenerating hepatocytes is 3.6% and decreases below 1% at 72 h after PH (Grisham, 1962; Parton and Garriott, 1997). To restrict the cell population to one cell division after treatment, co-treatment with cytochalasin B could be considered. It would, however, be important to consider possible interactions between test chemical and cytochalasin B. Therefore we believe that it is acceptable to perform the assay without co-treatment of cytochalasin B as long as rats at 4 weeks of age are used.

The AO-DAPI staining method, which was originally developed for the testis micronucleus assay (Noguchi, 1997), was efficient for analysis of micronuclei in cytoplasm of hepatocytes. This novel staining method gave clearer distinction of

micronucleus, nucleus, and cytoplasm than the single fluorescent staining with either AO or DAPI. To evaluate the practicability of the staining method, 12 laboratories participated in the collaborative trial and obtained similar MNHEP frequencies after treatment with 40 mg/kg DEN. This result indicated that the new staining method is powerful even for novice users of the liver micronucleus assay.

We chose the 4-week-old rat for the liver micronucleus assay based on our present results and also on the knowledge of age-related changes in metabolic enzyme profiles: Cytochrome P-450 content in young rats is similar to that in adult rats (Imaoka et al., 1991); there is no major difference between 30-day-old and 100-day-old rats in the activity of hexobarbital hydroxylation, *N*-demethylation of ethylmorphine, *O*-demethylation of *p*-nitroanisole or hydroxylation of aniline (Furner et al., 1969). P-450-1A2, 2A1, 2B1, 2B2, 2E1, 3A1, and 3A2 activity levels reach a maximum at about 30 days of age, thereafter, the levels of these P-450 species plateau in the liver due to growth hormone action. Conversely, P-4502C7, 2C11, 2C12, and 2C22 are expressed rapidly after 30 days of age (Kato and Yamazoe, 1992). Thus, a compound which is principally activated by P-4502C family, may not be easily detected by this assay. Further confirmation of this notion is being pursued.

Based on the present outcomes using DEN, we propose the following standard protocol for the young rat liver micronucleus assay:

Animals: Young rats up to 4 weeks old.
Route: Oral or intraperitoneal administration.
Chemical dosing: Single, or repeatedly if necessary.
Sampling time: 3–5 days after the last treatment.
Hepatocyte preparation: Collagenase perfusion method.
Staining: AO-DAPI double staining.

An extensive collaborative study for validation of the present method is still ongoing organized by The Collaborative Study Group of the Micronucleus Test – Mammalian Mutagenicity Study Group/Japanese Environmental Mutagen Society (CSGMT-MMS/JEMS). This involves evaluating micronucleus induction in young rat liver cells by hepatocarcinogens and some other related chemicals. The degree of validation will determine the extent to which the present method becomes recognized as a useful tool for evaluating genotoxicity of chemicals in the rat liver.

## References


Angelosanto FA: Tissues other than bone marrow that can be used for cytogenetic analysis. Environ molec Mutagen 25:338–343 (1995).

Braithwaite J, Ashby J: A non-invasive micronucleus assay in the rat liver. Mutat Res 203:23–32 (1988).

Cliet I, Fournier E, Melcion C, Cordier A: In vivo micronucleus test using mouse hepatocytes. *Mutat Res* 216:321–326 (1989).

Committee on the Mutagenicity of Chemicals: Guidance on a Strategy for Testing Chemicals for Mutagenicity. (London 2000).

Furner RL, Gram TE, Stitzel RE: The influence of age, sex and drug treatment on microsomal drug metabolism in four rat strains. *Biochem Pharmacol 18:* 1635–1641 (1969).

Hayashi M, Morita T, Kodama Y, Sofuni T, Ishidate M Jr: The micronucleus assay with mouse peripheral blood reticulocytes using Acridine Orange coated slides. Mutat Res 245:245–249 (1990).

Higgins GM, Anderson RM: Experimental pathology of the liver. I. Restoration of the liver of the white rat following partial surgical removal. Arch Pathol 12:186–202 (1931).

Imaoka S, Fujita S, Funae Y: Age-dependent expression of cytochrome *P*-450s in rat liver. Biochim biophys Acta 1097:187–192 (1991).

Grisham JW: A morphologic study of deoxyribonucleic acid synthesis and cell proliferation in regenerating rat liver: autoradiography with thymidine-$H^3$. Cancer Res 22:842–849 (1962).

Kastenbaum MA, Bowman KO: Tables for determining the statistical significance of mutation frequencies. Mutat Res 9:527–549 (1970).

Kato R, Yamazoe Y: Sex-specific cytochrome P450 as a cause of sex- and species-related differences in drug toxicity. Toxicol Lett 64/65:661–667 (1992).

Mereto E, Brambilla-Campart G, Ghia M, Martelli A, Brambilla G: Cinnamaldehyde-induced micronuclei in rodent liver. Mutat Res 322:1–8 (1994).

Morita T, Asano N, Awogi T, Sasaki Y, Sato S, Shimada H, Sutou S, Suzuki T, Wakata A, Sofuni T, Hayashi M: Evaluation of the rodent micronucleus assay in the screening of IARC carcinogens. Groups 1, 2A and 2B. The summary report of the 6th collaborative study by CSGMT/JEMSMMS. Mutat Res 389:3–122 (1997).

Noguchi T: The development of testis micronucleus test (Abstract). 26th JEMS, Hatano, 92 (1997).

Parton JW, Garriott ML: An evaluation of micronucleus induction in bone marrow and in hepatocytes isolated from collagenase perfused liver or from formalin-fixed liver using four-week-old rats treated with known clastogens. Environ molec Mutagen 29:379–385 (1997).

Rossi AM, Romano M, Zaccaro L, Pulci R, Salmona M: DNA synthesis, mitotic index, drug-metabolising systems and cytogenetic analysis in regenerating rat liver. Mutat Res 182:75–82 (1987).

Roy B, Das RK: Evaluation of genotoxicity of clofazimine, an antileprosy drug, in mice in vivo. II. Micronucleus test in bone marrow and hepatocytes. *Mutat Res 241:169–173 (1990).*

Sawada S, Yamanaka T, Yamatsu K, Furihata C, Matsushima T: Chromosome aberrations, micronuclei and sister-chromatid exchanges (SCEs) in rat liver induced in vivo by hepatocarcinogens including heterocyclic amines. Mutat Res 251:59–69 (1991).

Sipes IG, Gandolfi AJ: Biotransformation of toxicans, in Amdur MO, Doull J, Klassen CD (eds): Casarett and Doull's Toxicology. The Basic Science of Poisons, pp 88–126 (McGraw-Hill, New York 1993).

Tates AD, Neuteboom I, Hofker M, Engelse L: A micronucleus technique for detecting clastogenic effects of mutagens/carcinogens (DEN, DMN) in hepatocytes of rat liver in vivo. Mutat Res 74:11–20 (1980).

Zhurkov VS, Sycheva LP, Salamatova O, Vyskubenko IF, Feldt EG, Sherenesheva NI: Selective induction of micronuclei in the rat/mouse colon and liver by *1,2-dimethylhydrazine*: a seven-tissue comparative study. Mutat Res 368:115–120 (1996).